LAPPEENRANTA UNIVERSITY OF TECHONOLOGY
LUT School of Energy Systems
Master's Programme in Energy Systems

Nishan Khadka

HEAT RECOVERY FROM FLUE GAS CONDESING AND OVERALL IMPACT ON CHP EFFICEINCY

Examiners: Professor Esa Vakkilainen
D.Sc. (Tech.) Juha Kaikko

ABSTRACT

LAPPEENRANTA UNIVERSITY OF TECHNOLOGY
LUT School of Energy Systems
Master's Degree Programme in Energy Systems

Nishan Khadka

Heat recovery from flue gas condensing and overall impact on CHP efficiency

Master's Thesis

2019

70 pages, 29 figures, 13 tables and 2 appendices

Examiners: Professor Esa Vakkilainen
D.Sc. (Tech.) Juha Kaikko

Keywords: FGC, heat pump, CHP, DH, spray tower, IPSEpro

This thesis paper investigates the flue gas condensing (FGC) and its integration in combined heat and power plant (CHP). FGC method utilizes the latent heat from flue gas and heat is released during condensation. It is considerable choice to increase the power plant efficiency and reduce the emission levels. The heat recovery from flue gas can be effectively achieved by the addition of heat pump or combustion air humidifier. The recovered heat could be utilized to increase district heat (DH) production or other industrial purposes.

Spray tower and heat pump are modeled in IPSEpro software for condensing and energy recovery and, modeling is entirely based on heat and mass transfer principle. The integration of FGC was carried out in 8 MW_{el} CHP plant, which is based on biomass fuel with 55% moisture content. Spray tower was modeled for two stage scrubbing with liquid water. Heat pump was modeled taking account only heat transfer in condenser and evaporator, and was simulated with different values of coefficient of performance (COP).

The simulation on CHP model integrated with spray tower and heat pump showed the increase in DH production and overall efficiency of CHP plant compared to stand-alone CHP model. The simulation also indicated the significant decrease in exhaust gas temperature and lower consumption of fuel. However, electricity consumed by heat pump and higher temperature supply to DH condenser resulted in lower electricity production.

ACKNOWLEDGEMENTS

I would like to express my gratitude to the teaching staff of LUT's School of Energy Systems for all the guidance and support during my wonderful life at University. First, I would like to thank Professor Esa Vakkilainen for providing me opportunity to write thesis on this interesting and exciting topic. Special thanks to D.Sc. Juha Kaikko and D.Sc. Jussi Saari for providing huge assistance and guidance to understand the IPSEpro software and continue my thesis.

I also feel grateful to my family for providing me love and support in every steps of my life. I would like to thank Sushan and Aroma, who provided crucial support and motivation to keep me calm and focused. In addition, I would like to thank all my friends who helped me to develop positive attitude through wonderful moments and inspiration.

TABLE OF CONTENTS

LIST OF ABBREVIATIONS

BAT	Best Available Techniques
BAT-AELs	BAT-Associated Emission levels
BREF	BAT Reference Document
BFB	Bubbling Fluidized Bed
COP	Coefficient of Performance
CFB	Circulating Fluidized Bed
DH	District Heating
DHC	District Heat Condenser
EC	European Commission
FAO	Food and Agriculture Organization
FGC	Flue Gas Condenser
FGD	Flue-Gas Desulfurization
GCV	Gross Calorific Value
GHG	Greenhouse Gas
IEA	International Energy Agency
LCA	Life Cycle Assessment
MDK	Model Development Kit
PSE	Process Simulation Environment
SCR	Selective Catalytic Reduction
SNCR	Selective Non-Catalytic Reduction
SPF	Seasonal Performance Factor

LIST OF FIGURES

LIST OF TABLES

1 INTRODUCTION

The global human activities in agriculture, energy, transport and industries have led to the depletion of natural resources and anthropogenic emissions causing global climate change. These activities have resulted in global warming of 1.0^{o}C above pre-industrial levels, and if this rate continues, the warming of 1.5^{o}C is expected to occur between 2030 and 2052. The mitigation measures for reducing greenhouse gases (GHGs), black carbon, sulphur dioxide, etc. from agriculture, waste and energy sector play vital role for limiting the warming of 1.5^{o}C by 2100 (IPCC, 2018).

Switching fossil fuels, development of renewable energy technologies, energy conservation and efficiency are vital to lower GHGs emissions and fulfilling the global energy demand. Bioenergy provides significant role in GHGs mitigation, however, development of sustainable and efficient systems are required to fulfill this role. Use of advanced conversion technology, sustainable cropping systems, residues and municipal wastes, bioenergy has emission reduction potential of 80 to 90% compared to than that of fossil energy (IPCC, 2011).

Modern bioenergy accounted for 70% share of renewable heat production in 2017 excluding the traditional biomass use. The major consumer of heat from biomass remains industry, which accounted for 8% of its total heat demand. Residential sectors and buildings accounted for approximately 32% of heat consumption from modern bioenergy (OECD/IEA, 2018). Cogeneration provides suitable choice for utilizing modern bioenergy to produce electricity and district heating by achieving lower environmental impacts and improving energy efficiency, energy supply, and cost efficiency (Werner, 2017).

In EU states, district heating contributed to 9% of total heat supply and biomass accounted for 16% of share in heat supply (EC, 2016). The main bioenergy supply for district heat supply in Finland in 2017 were forest wood (18%), peat (14%), industrial wood residues (11%), and other biofuels (8%). Heat recovery in heat pump accounted for 9% same year (Energiateollisuus, 2018).

To further increase the energy efficiency and reducing emissions, heat recovery technique such as flue-gas heat condenser can be implemented in cogeneration cycle. Flue-gas heat condenser is a heat exchanger where flue gas temperature is lowered to water vapor dew point temperature to recover both sensible and latent heat by the use of either tube condenser or direct contact with cooling water, however, condensation also dependent on the moisture content of fuel (European Commission, 2017). The temperature of exhaust flue gas is generally around 150^{o}C and contains 15% to 40% of fuel heat content. With flue-gas condenser, the exit temperature could be reduced to 40 to 50^{o}C, which leads to the increase in thermal efficiency of plant, energy saving of about 15% and reduction in carbon dioxide emissions (Terhan & Comakli, 2016). The condensation of flue gas allows it to dissolve complete or partial constituents of flue gas such as nitrous oxides, sulphur oxides, dust, etc. and contribute to reduction of emissions to the environment (Defu, et al., 2004).

Half of the total energy consumed in Europe is estimated to direct towards heating and cooling. Therefore, optimizing and maximizing the efficiency of heat supply could reduce the energy consumption, increase the security of supply and contribute to decarbonize the energy sector (David, et al., 2017). Integration of large-scale heat pumps in district heat network limits the energy and heat losses by utilizing the waste heat through closed compression cycle. However, cost of the equipment and utilization of extra energy (electricity or heat) could be disadvantage.

Integration of flue gas condensing unit and heat pump could significantly increase the district heating efficiency of cogeneration plants without additional demand of fuel supply and reducing emissions to atmosphere. In flue gas condensing systems in cogeneration plants, the return temperature from district heat network plays an important role in heat production. The return temperature should be lower than the dew point of the flue gas in order to recover energy from condensation of flue gas. On the other hand, the electricity production could be lowered due to the higher temperature supply to district heat condenser that results in expansion of steam from backpressure turbine to a higher pressure (Cuadrado, 2009).

The present study provides background information on biomass use in heat and electricity production, flue gas cleaning technologies and extracting surplus heat from flue gas. Spray tower scrubber and heat pump applications are studied in detail for utilizing condensing heat from flue gas to increase the district heat efficiency.

2 BIOMASS FUEL AND COMBUSTION

With the increase in global warming and climate change scenario induced by fossil-based fuel, the use of biomass-based fuels have been increasing in recent years. Biofuels contributed to approximately 9.7 percent share of total primary energy supply whereas contributed to 1.9 percent share in world electricity production and 4 percent in production of heat in 2015 (IEA, 2018). Currently, solid biofuel is the fourth largest renewable source for electricity production after hydro, wind and solar technologies.

Unlike fossil fuels, biomass fuel have lower energy density and higher moisture content, low bulk density and higher oxygen levels. According to origin, biomass fuel is mostly categorized on three basis: wood fuels, agro-fuels and municipal by-products as shown in Table 1 below.

Table 1. Types of biomass according to origin (FAO, 2004).

Wood biomass	Direct and Indirect wood fuels
	Recovered wood fuels
	Wood derived fuels
Agricultural and forest residues	Fuel crops
	Agricultural and animal by-products
	Agro-industrial by-products
Municipal by-products	Municipal waste
	Sewage sludge, landfill gas, etc.

Various processes and technologies are available currently to use different biomass feedstock for the production of useful energy for electricity, heat and transport. The production of heat and electricity from wood biomass, agricultural residues, ethanol from sugarcane and maize and biodiesel from rapeseed, soybean and other oil crops are common pathways of biomass to energy use. However, the biomass conversion to useful energy consists of many processes such as production and harvesting of biomass, pretreatment to change chemical properties, etc. The trend of modern bioenergy in transport, heat and electricity is presented in Figure 1.

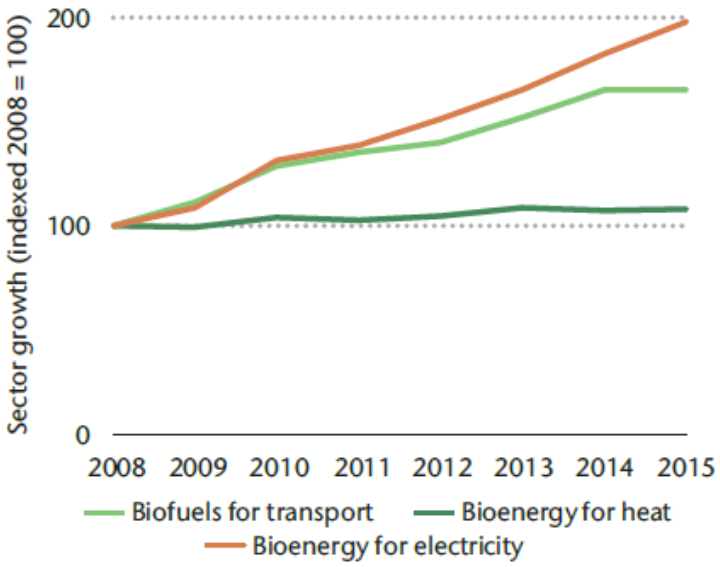

Figure 1. Trend of modern bioenergy by sector (OECD/IEA, 2017).

The consumption of biomass for heat sector is largest but with respect to the sector, the consumption of bioenergy for electricity and biofuels for transport is growing faster (OECD/IEA, 2017). The highest use of biomass for heat use worldwide is open fires and traditional stoves for cooking. It is also used for heat use in pulp and paper industry, food and chemical industries. Northern European countries use significant fraction of biomass to fulfill heating demand for household purposes (IEA/FAO, 2017).

The worldwide production of conventional biofuels was approximately 4% share for road transport fuel in 2016 and the growth is slow as compared to electricity use. This is explained by low government policies to promote biofuels and lower oil prices that causes market specific challenges. Solid biomass and wastes have been the main contributor for bioenergy energy production with over 70% share among biomass fuels. However, the electricity generation from biomass is not popular worldwide with about 90% capacity located in only 26 countries as per statistics in 2016 (OECD/IEA, 2017). The cost efficiency of biomass-based power plant is dependent critically on the plant scale, availability and quality of feedstock (IEA/FAO, 2017).

The main driver for promoting the use of biomass for heat and electricity has been the reduced lifecycle GHG emissions compared to fossil fuel use. The lifecycle GHG emissions from bioenergy excluding land use change and fossil fuel is provided in Figure 2.

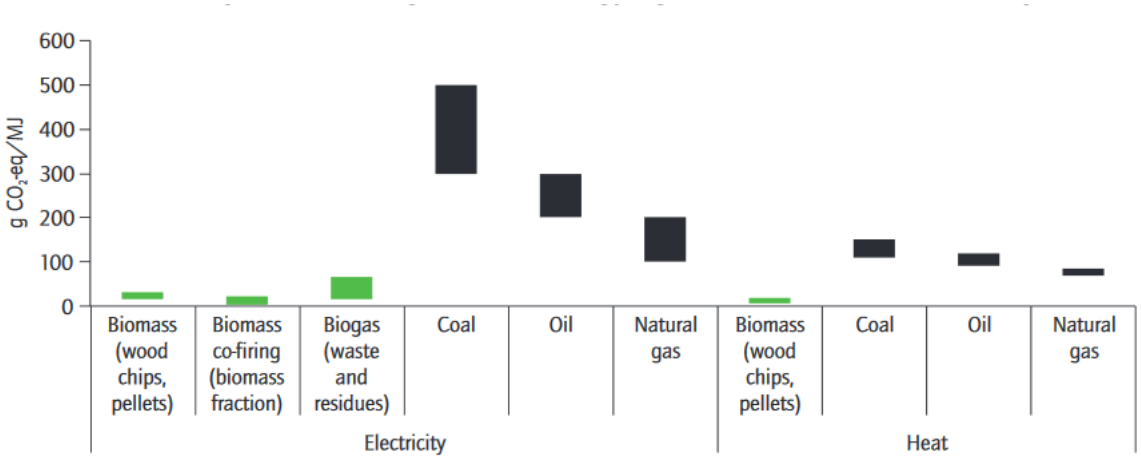

Figure 2. Life cycle GHG emissions from bioenergy excluding land use change and fossil fuel (IPCC, 2011) (Cherubini, et al., 2011).

Although the lifecycle assessment (LCA) and emission guidelines for CO_2 emissions from biomass fuel excludes the emission from conversion and considers it neutral due to the absorption from atmosphere during growth, there has been questions regarding this assumptions. The important measure for ensuring GHG reduction through bioenergy is good forest and agricultural management practices, however, other sustainability issues should be considered such as biodiversity, soil fertility, water use, employment, health impacts, etc. (IEA, 2012).

2.1 Biomass fuel properties

The main biological characteristics of wood biomass are cellulose, hemicellulose and lignin, and cellulose being the major constituent and dominant role in combustion. Organic and inorganic materials such as mineral, salt and water are present lower in wood biomass whereas, these material are found in higher amount in rice and wheat straw (Sullivan & Ball, 2012). The composition of wood biomass is categorized into four parts: fixed carbon, ash content, volatiles and moisture content as shown in Figure 3 below.

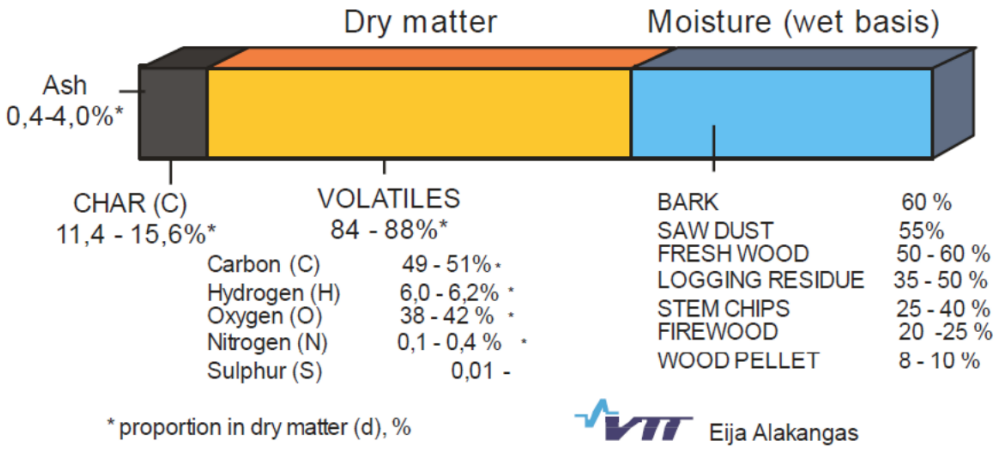

Figure 3. Typical composition of wood biomass (Alakangas, et al., 2016).

The moisture content is high in solid biofuels and the present of carbon, hydrogen and oxygen is high. It also depends upon type of biomass and its handling process such as pre-treatment, drying, etc. The moisture content was found to highest in bark up to 70% and waste wood has less moisture. On the dry basis, volatiles made up to 80-90% in the wood biomass (Alakangas, et al., 2016). Fuel with high volatile contents have high combustion efficiency in low temperatures than low volatile contents. In addition, higher volatile contents also lead to the rapid and complete ignition. The ash content of the dry basis fuel is defined as weight percentage, typical value for wood biomass is 0.4%, and coal is 11% (Huhtinen, et al., 1994).

The process of biomass utilization in combustion technologies for electricity generation is affected by the chemical composition of solid biomass. The moisture content, gross calorific value (GCV), net calorific value (NCV), bulk density and energy density for different biomass fuels is provided in Table 2 below.

Table 2. Key properties of biomass fuels (Kaltschmitt & Hartmann, 2001).

Biomass fuel	Moisture content (wt.%) (wb)	GCV (MJ/kg) (db)	NCV (MJ/kg) (wb)	Bulk density (kg/m^3) (wb)	Energy density (MJ/m^3)
Wood pellets	10	19.8	16.4	600	9,840
Woodchips-hardwood	50	19.8	8	450	3600
Woodchips-softwood	50	19.8	8	350	2,800
Bark	50	20.2	8.2	320	2,620
Saw dust	50	19.8	8	240	1,920

2.2 Combustion technologies

2.2.1 Basics of Steam cycle

For steam power plants, the Rankine cycle have been considered ideal cycle. Although Carnot cycle is most efficient cycle, which operates between two temperature limits, it is not suitable cycle for power cycles. It limits the maximum temperature in the cycle and hence the thermal efficiency. Another issue is that, it needs isentropic compression of liquid-vapor mixture to a saturated liquid, which is not easy to control the condensation process, and it is not feasible to design the compressor that can handle two phases (Cengel & Boles, 2015).

In the Rankine cycle, steam is superheated in the boiler and condensate completely in the condenser. The ideal Rankine cycle and basic power plant cycle is provided in Figure 4. The efficiency of Rankine cycle can be increased by either increasing the average temperature of heat supplied or decreasing the average temperature of rejected heat (Borgnakke & Sonntag, 2012). The four process provided in Figure 4 are:

1-2: Isentropic compression in the pump

2-3: Constant pressure heat addition in the boiler

3-4: Isentropic expansion in the turbine

4-1: Constant pressure heat rejection in a condenser

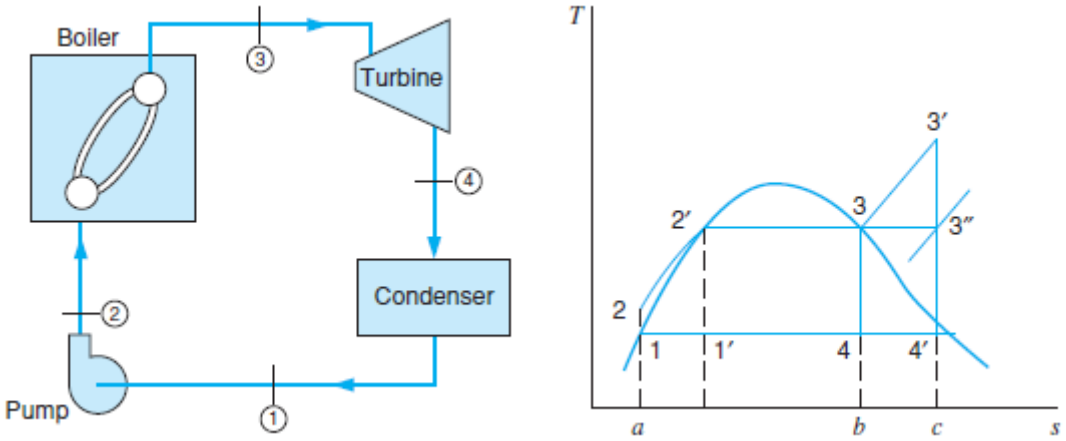

Figure 4. Basic steam power plant cycle and Rankine cycle (Borgnakke & Sonntag, 2012)

For industrial production of heat and power, different combustion technologies are used. Based on firing process, biomass is combusted in different types of boilers: direct, grate, fluidized bed and recovery boiler. Direct firing is the cheap replacement technology for coal and are used for firing biomass pellets in power plants of size up to 60 MWth. Due to the low investment cost, availability of remote operation, fast start up, etc. direct firing have been popular these days (Vakkilainen, 2017). Grate firing and fluidized bed combustor are the most common combustion technologies for solid biomass fuels.

2.2.2 Grate firing

Grate firing is the oldest method of firing and is popular choice for combustion of biomass solid fuels for the size of plant about 10 MWth (Vakkilainen, 2017). Grates firing are mostly categorized into stationary and moving. Travelling grate, reciprocating grate, vibrating grate are the main types of moving or mechanical grates (Yin, et al., 2008). Figure 5 shows the combustion stages of biomass fuel in typical mechanical grate firing. The stages are 1) fuel feed, 2) drying, 3) devolatilisation of fuel, 4) char combustion, 5) ash formation and 6) primary air feed.

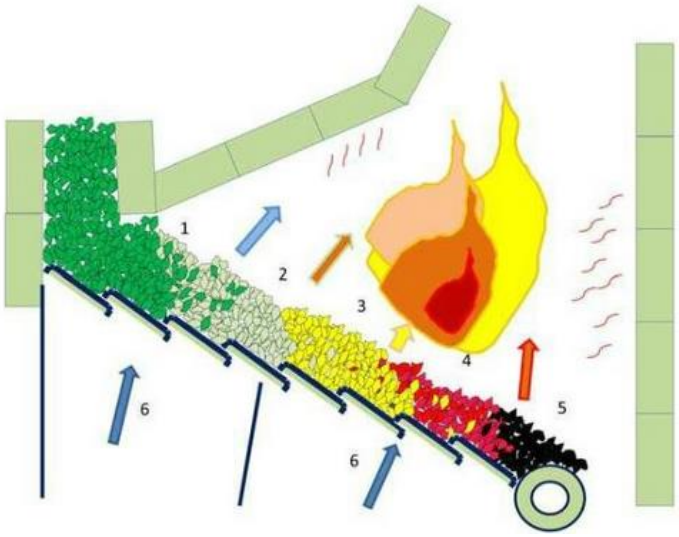

Figure 5. Combustion stages of biomass fuels in mechanical grate firing (Vakkilainen, 2017).

The biomass fuels for grate firing are mainly categorized into dedicated energy crops (hard wood trees, herbaceous crops, etc.) and waste products (wood materials such as wood chips, saw dust, bark and crop residues such as rice straw, husks, etc.) (Yin, et al., 2008). The achieved heat loading of bark and wood in the mechanical grate is 0.4 MW/m^2 with 60% moisture content and 0.8 MW/m^2 with 30% moisture content (Vakkilainen, 2017).

One of the big challenges in Grate firing boilers is the incomplete combustion of the biomass fuel, which can result to emission problems such as high levels of unburned carbon in fly ash and higher emissions of PCDD/PCDF. The reason for the incomplete combustion is fuel mixing, which can be reduced by the integration of advanced air supply systems, adequate residence time at high temperature and lowering the total excess air (Yin, et al., 2008).

2.2.3 Fluidized bed combustion

Fluidized bed combustion is the popular choice for large power production (>50 MWth) because of high combustion efficiency, lower nitrogen oxides (NO_x) emissions, possibility of simultaneous use of several fuels, and easy Sulphur removal process. There are two main types of fluidized bed combustion: bubbling fluidized bed boiler (BFB) and circulating fluidized bed boiler (CFB). The CFB boilers are used in the plant size greater than 100 MWth where as BFB boilers are used in less than that (Vakkilainen, 2017). Figure 6 shows the operating principle of different fluidization: fixed bed, BFB, and CFB where ε is the ratio of empty volume in the bed.

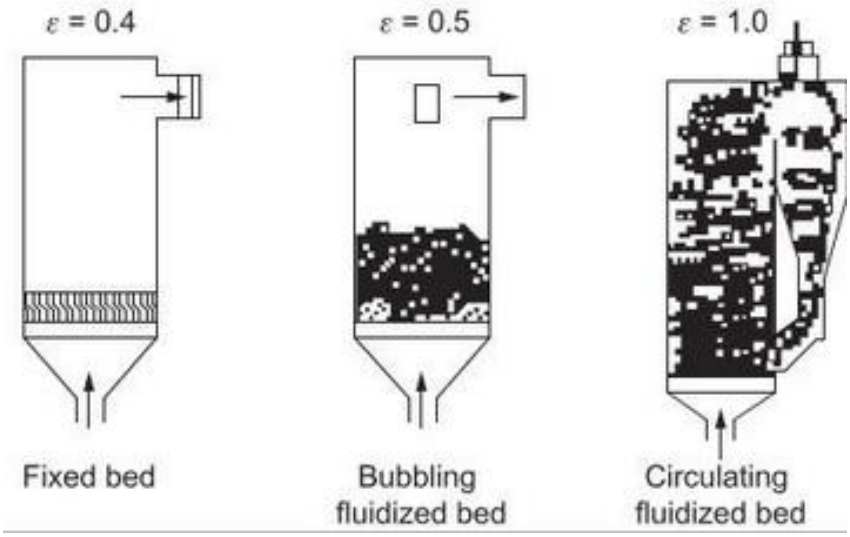

Figure 6. Operating principle of different fluidization technologies (Vakkilainen, 2017).

The working principle of fluidizing bed is to blow air in the bed made from fine sand and ash that gains the velocity due to air and behaves like a fluid due to the increased velocity of air. The fuel is then mixed with this fluid at the bottom of the furnace. This fluidization principle makes it beneficial for efficient fuel combustion and maximum heat transfer between the heat transfer surfaces and the gas due to the continuous contact of fluid with the heat transfer surface (Vakkilainen, 2017).

Fluidized bed boilers have higher fuel flexibility and is suitable of most of the biomass fuels. BFB has the fuel combustion efficiency of 90-96% efficiency whereas CFB has efficiency of 95-99.5% due to better gas-solid mixing, higher combustion rate and the continuous recirculation of unburnt carbon particles in the furnace base (Basu, 2015).

The CFB boiler is more efficient than BFB in capturing Sulphur due to the less need of stoichiometric amount of sorbent in the CFB although both have similar Sulphur removal efficiency of 80-90%. CFB boilers have lower NO_2 emissions, which is about 50-150 ppm (Hiltunen & Tang, 1988). Due to the higher efficiency of mixing, CFB boiler emits less carbon monoxide (CO) and C_xH_y gases, however, emission level for nitrous oxide (N_2O) are higher than pulverized coal-fired boilers. One of the drawbacks of fluidized bed boilers is the higher consumption of limestone than flue-gas desulfurization (FGD) which is 3-5 times is BFB and 2 times in CFB which results in higher production of solid waste such as gypsum (Basu, 2015).

2.3 Flue Gas emissions

2.3.1 Flue gas composition

The composition of biomass varies from species to species which determines the flue gas composition. Flue gas is also determined by type of power plants and boiler used. In order to study the flue gas emissions, it is important to study about chemical composition of biomass. The properties such as volatiles, moisture, ash content, trace elements, etc. of three different biomass fuels are provided in Table 3 based on as-received (ar) and dry basis (db). In terms of trace metal and nitrogen contents, agricultural fuels and herbaceous biomass fuels can be significantly different from woody biomass (Jones, et al., 2014).

Table 3. Proximate and Ultimate analysis of wood, bark and straw pellets (Qin & Thunman, 2015).

Properties	Wood pellet	Bark pellet	Straw pellet
Proximate analysis			
Ash (ar) (Wt. %)	0.41	3.39	7.13
Volatiles (ar) (Wt. %)	74.14	65.66	66.40
Moisture (ar) (Wt. %)	8.40	8.26	11.03
Fixed Carbon (ar) (Wt. %)	17.05	22.69	15.44
LHV (ar) (MJ/kg)	17.13	17.71	14.35
LHV (db) (MJ/kg)	18.70	19.31	16.13
LHV (dry and ash free basis) (MJ/kg)	18.79	20.05	17.54
*Ultimate analysis (ar) (*Wt. %)			
C	45.94	48.35	38.88
H	5.50	5.28	5.44
O	39.65	34.26	36.75
N	0.08	0.43	0.70
S	0.02	0.02	0.01
Ca	0.11	0.80	0.23
K	0.03	0.19	0.36

The burning of biomass results in emission of carbon monoxide, organic compounds and smoke caused by the presence of carbon, hydrogen and oxygen content in biomass. Other emissions are unburned hydrocarbons, volatiles, Polycyclic Aromatic Hydrocarbons (PAH), Nitrogen oxides (NO_x), Sulphur, chlorine compounds and dioxins. Size of combustion units can affect the amount of emissions. Small combustion plants with no control system, poor mixing and short residence times can cause higher pollution levels. Combustion in large plants with carefully controlled form low pollutant levels (Jones, et al., 2014).

For appropriate combustion and gas-cleaning technologies, the choice of fuel with suitable ash content is essential. Ash content of fuel determines the fly ash formation, ash deposition, ash storage and disposal. Bark and straw have higher ash content whereas wood has lower amount of ash. However, grate and fluidized bed boilers are suitable for fuels with higher ash content (Obernberger, et al., 2006). The emission levels from different biomass combustion source based on dried flue gas composition is provided in Table 4.

Table 4. Emission levels from different source of biomass combustion (Jones, et al., 2014).

Unit types	Residential boiler (2-10 kW)	Fixed Grate (20 kW-2.5 MW_{th}	Travelling Grate (150 kW-15 MW_{th})	Fluidized bed (100 MW_{th})	Co-firing (GW_{th})
Fuel	Wood chips, Miscanthus	Most biomass	Straw	Most biomass	Most biomass
NO_x (mg/Nm^3)	100-500	150-400	150	150	250
Particulate (mg/Nm^3)	20-100	1	1	5	15
VOC (mg/Nm^3)	10	10	10	15	0.1
CO (mg/Nm^3)	250-800	130-600	150	5	100
Reference O_2 level (Mol %)	6	11	11	11	6

The NO_x emissions represented in Table 4 depends on the fuel nitrogen content. The data represents the average value for combustion cycle for each unit. All the combustion units except residential boiler is assumed to have pollution control equipment.

Nitrogen oxides have significant effect on acid rain, ozone formation and health effects. These are formed by either oxidation of atmospheric nitrogen gas in high temperature or oxidation of nitrogen present in the fuel. Sulphur and chlorine amounts are lower in biomass fuels. Both are released partly during devolatilisation and released during the combustion of the char by evaporation or sublimation of chlorides, hydroxides or oxides. Depending on temperature, chlorine (Cl) is released as potassium chloride (KCl) and hydrogen chloride (HCl) which leads to the corrosion of furnace walls. During combustion process, sodium, calcium and silica are released forming inorganic particles, which is either released in atmosphere as pollutants or deposited in wall of furnace causing problems like corrosion, fouling and slagging (Jones, et al., 2014). Vapors of volatile compounds can react on existing fly ash particles surfaces or condensate when flue gas is cooled in the convective heat exchanger (Obernberger, et al., 2006).

2.3.2 Cleaning technologies

Flue gas from burning biomass have significant effect on weather, climate, environment and human health. The gas cleaning is mostly divided in four parts: removal of dust or particles, removal of NO_x, removal of water-soluble gases (SO_2, HCL, HF, and NH_3) and removal of toxic substances like dioxins and mercury. There are three main physical process involving cleaning of flue gas: wet method, dry method, and hybrid method. Wet method uses liquid agent to clean the flue gas whereas, dry method uses techniques such as inertia principle, permeability principle, etc. Wet methods includes wet scrubbers, electrified wet scrubbers, wet electrostatic precipitator, wet scrubber with condensation, etc. Dry methods include electrostatic precipitators, fabric filters, electrified sand bed filter, cyclones and so on. Some of the hybrid methods include electrocyclone and novel swirl cyclone (Singh & Shukla, 2014).

Primary method of reduction of NO_x emission can be achieved to 30-50% compared to conventional combustion by air staging combined with air-oxygen ratio (λ) around 0.7, temperature between 900-1100^oC and residence time of 0.5 seconds of flue gas in the combustion chamber (Obernberger, et al., 2006). Other primary methods of NOx removal are flue gas recirculation in furnace, reduced air preheat, low excess air, and fuel staging. The secondary processes are selective catalytic reduction (SCR) operated between high flue gas temperatures and selective non-catalytic reduction (SNCR) operated between low flue

gas temperatures where ammonia (NH_3) is injected into flue gas to produce diatomic nitrogen (N_2) and water (Wendt, et al., 2001).

Cyclones, conventional wet scrubbers, fabric filters and electrostatic precipitator are the common method of removal of dust/particles from flue gas. Cyclones are beneficial as pre-cleaning device for the particles size greater than 10µm aerodynamic diameter (Lee, et al., 2008). As Sulphur contain is very low in biomass fuels, it can be partly captured in biomass ash by alkaline-earth fractions (Jones, et al., 2014). The process of removing Sulphur from flue gas in thermal power plants is called Flue gas desulphurization (FGD) and the typical chemical reactions for FGD is provided equations (1) and (2) (Kohl & Nielsen, 1997).

$$2NaOH + SO_2(gas) \rightarrow Na_2SO_3(solid) + H_2O(liquid) \quad (1)$$

$$Na_2SO_3(liquid) + \frac{1}{2}O_2(gas) \rightarrow Na_2SO_4(solid) \quad (2)$$

The different types of absorbers for wet FGD are spray tower, packed bed tower, turbulent bubble bed reactor, etc. Due to collective efficiency and wide range of operating temperature, Electrostatic precipitator are most extensively used as pollutant control systems. Other water-soluble gases such as HCl, HF, NH_3, etc. are removed by either wet methods or dry absorption. Dioxins and mercury are removed by the introduction of activated carbon sorbents in flue gas (Singh & Shukla, 2014). However, due to high cost of these activated carbons, new alternative of brominated ash, which is industrial waste, and was found to capture mercury effectively up to 390^{o}C, has been proposed (Bisson, et al., 2013). Scrubbers are discussed in more detail in chapter 2.5.2.

2.3.3 Influence of high humid flue gas emissions

Flue gas with high humidity discharging from power plants have several impacts on environment. Its effect on smog weather, water saving and boiler thermal efficiency and the corrosion of flue and chimney are the main challenges. The high humidity condition of flue gas increases the level of humidity in lower atmosphere, and is unfavorable to the pollutants diffusion, which can have impact on local climate surrounding the plant (Shuangchen, et al., 2017).

The secondary transformation of air pollutants are influenced by the flue gas emissions with high humidity. In this condition, aerosol particles absorb moisture from flue gas in the atmosphere, which makes pollutants like SO_2 and NO_x to enter aerosol through water film inside it. As a result, the properties of aerosol are changed and is acidic which precipitates on the surface as acid rain. Besides, high humidity from flue gas accelerates the hygroscopic growth of aerosol, which in result change its optical characteristics. This results in the reduction of the atmospheric visibility (Shuangchen, et al., 2017).

Large amount of latent and sensible heat are released in flue gas. It has been concluded that, the wet flue gas discharged from cooling tower in thermal power plant has almost two times more energy compared to the electric energy generated by it (Hanna, 1976). In addition, high humidity is opposing to water conservation and reuse of heat in power plant itself due to release of much of latent heat of vaporization (Shuangchen, et al., 2017).

At high humid environment of flue gas and low temperature condition, corrosive gases react with water to form acid solution such as sulfuric acid, nitric acid, etc. which leads to pitting, crevice, stress corrosion, etc. The presence of high moisture allows the retention time of acid pollutants, accelerates the formation of corrosive substances that leads to the increased corrosion of chimney (Shuangchen, et al., 2017). In addition, the occurrence of gypsum rain is highly influenced by the high amount of wet flue gas emissions that causes the change in local climate condition (Zhuang, et al., 2015).

Several countermeasures are available in order to solve the impact from the high humidity in flue gas. Flue gas heating, recovery of water from flue gas, removal of sub-micron particulates, etc. are the effective countermeasures (Shuangchen, et al., 2017). Recovery of water from flue gas is studied in more detail in this research paper.

2.4 BAT-AELs for combustion plants

The best available techniques (BAT) reference document (BREF) for combustion plants has been reported by European Commission (EC) as required by Article 13(1) of Directive 2010/75/EU on Industrial Emissions for the aim of integrated pollution prevention and control. The efficiencies of various fuels and different size combustion plants, pollution removal techniques, emission criteria, etc. are being defined in BREF. Table 5 indicates the BAT-associated emission levels (BAT-AELs) for the new combustion plants for solid biomass/peat.

Table 5. BAT-associated emissions levels (BAT-AELs) for new plants from the combustion of solid biomass and/or peat (European Commission, 2017).

Yearly average (mg/Nm^3)	Plant size (MWth)		
	<100	100-300	≥300
NOx	70-150 ([1])	50-140	40-140
SO_2	15-70	<10-50	<10-35
Particles	2-5	2-5	2-5
CO ([1])	<30-250	<30-160	30-80
HCl ([2]) ([3])	1-7	1-5	1-5
Hg	<0.001-0.005	<0.001-0.005	<0.001-0.005
HF ([4])	<1	<1	<1

([1]) The BAT-AELs do not apply to plants operated <1500 h/yr.

([2]) The maximum range of BAT-AEL for new plants is 15 mg/Nm^3 and 25 mg/Nm^3 for existing plants and this range applies to plants where burning fuels have average chlorine content is ≥0.1 wt-% (dry) or existing plants co-combusting sulphur-rich fuel with biomass or plants using alkali chloride-converting additives.

([3]) The maximum limit of BAT-AEL is 15 mg/Nm^3 for new plant operated <1500 h/yr.

([4]) These levels are indicated for the plants operated <500 h/yr.

The BREF has also stated the BAT-AEL for the direct discharges from flue gas treatment to a receiving water body, which is shown in Table 6. Different BATs have been used to control the waste of flue gas treatment. Precipitation and crystallization are the secondary techniques to avoid the dilution of metals and metalloids, sulphate (SO_4^{2-}) and fluoride (F^-). Anoxic/anaerobic biological treatment are other examples of secondary treatment for mercury (Hg) nitrate (NO_3^-) and nitrite (NO_2^-) (European Commission, 2017).

Table 6. BAT-AELs for the direct discharges from flue gas treatment to water bodies (European Commission, 2017).

Component	Daily average (mg/l)
Chemical oxygen demand (COD)	60-150 ([1]) ([2]) ([3])
Total organic carbon (TOC)	20-50 ([1]) ([2]) ([3])
Total suspended solids (TSS)	10-30
Fluoride (F^-)	10-25 ([3])
Sulphide (S^{2-})	0.1-2.0 ([3])
Sulphate (SO_4^{2-})	1300-2000 ([3]) ([4]) ([5]) ([6])
Sulphite (SO_3^{2-})	1-20 ([3])

([1]) BAT-AEL applies for either TOC or COD.

([2]) The daily average amount is applied after subtracting intake load.

([3]) This amount is only applied to the water from FGD.

([4]) If the calcium compounds are used in flue gas treatment, then only these limits are applied.

([5]) If the wastewater is highly saline where chloride concentrations are ≥5 g/l, then this higher limit of BAT-AEL does not apply.

([6]) If the wastewater is discharged to sea or high saltwater bodies, then this daily average limit does not apply.

2.5 Flue gas condensing

Flue gas from burning biomass contains high moisture level. The energy content of the fuel decreases and latent heat content rises when the fuel moisture level increases. Based on fuel, the flue gas can have 15-40% of the total energy content in the fuel (Defu, et al., 2004). Condensing heat exchanger is an efficient way of recovering moisture from flue gas. By lowering the flue gas temperature below dew point of the water, both latent heat due to condensation and sensible heat could be recovered (Selivanovs, et al., 2017).

Condensing of flue gas can be achieved by the use of two physical methods: condensing scrubber or tube condenser. Condensing scrubber consists of spray tower where flue gas gets physical contact with scrubbing liquid or water. In tube condenser, cold water flows through the tube and flue gas gets in contact with cold tube for heat transfer and condensation of water vapor. Condensing scrubbers have high efficiency in flue gas cleaning than in tube

condensers. In addition, tube condensers need prewashing unit to clean the flue gas beforehand to avoid the corrosion inside tube condenser (Uotila, 2015).

The gas-vapor mixture in the heat condenser is considered saturated when the water begins to condensate, which means that the gas mixture holds the maximum possible amount of moisture at that pressure and temperature. However, the dew point of the water depends on the volumetric water percentage share in the flue gas as shown in Figure 7. It is calculated that, the dew point of water increases with the volumetric share of water in the flue gas (Samuelson, 2008). However, not only water, flue gas will also condense with their corresponding dew points.

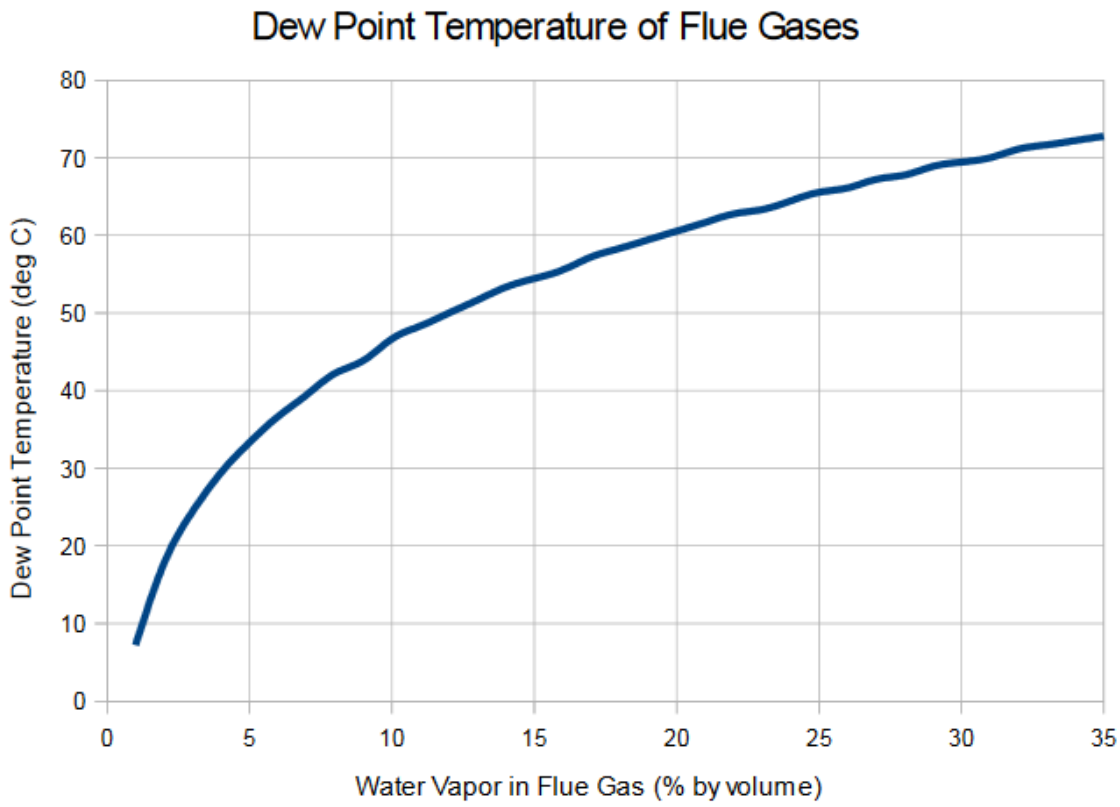

Figure 7. Relation between dew point temperature of water and volumetric percentage of water in flue gas (Engineering ToolBox, 2010)

The boiler load has inverse relation with specific heat energy recovered. When boiler load increases, recovered energy from flue gas per unit of heat produced decreases due to the condensation limitations. Therefore, it is vital to dimension the flue gas-condensing unit to the boiler capacity and load for effective heat recovery (Blumberga, et al., 2011).

Figure 8 represents the balance of heat fluxes in the condensing heat exchanger. However, it is a complex phenomenon due to the simultaneous presence of heat/mass transfer of water vapor and acids in the presence of non-condensable gases (Jeong, et al., 2010). In addition, the return temperature plays a vital role for the use of waste heat recovery in the heating system. It is calculated that the efficiency improvement of heat condenser would be 2.12% to 5.76% when the return temperature is between 40.8 - 53.3ºC (Defu, et al., 2004).

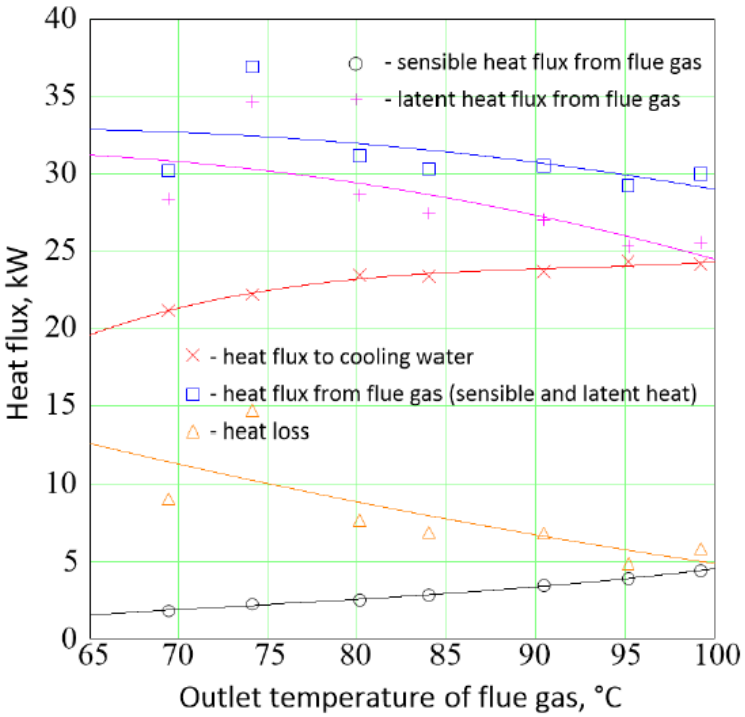

Figure 8. Example of heat flux balance in flue gas condenser (Szulc & Tietze, 2017).

In Figure 8, the blue line represents the total heat flux transferred by flue gas which is total of sensible heat flux (black line) resulting from cooling flue gas and latent heat flux (pink line) resulted from the condensation process of moisture in flue gas. The heat balance in chimney is provided in following equation (3) (Cuadrado, 2009).

$$Q_{latent} + Q_{sensible} = Q_{recovered} + Q_{losses} \quad (3)$$

2.5.1 Factors affecting energy recovery

Various factors have effect on the total energy recovered from the FGC. The three main factors are exhaust gas, district heating water and heat exchanger. The chemical composition of gases and moisture content in the gases, which is directly related to fuel, and temperature

of exhaust gas plays vital role in total energy recovered from flue gas. The flow rate and return temperature of district heating water and heat exchanger are another major factors for determining total energy recovered. The flow rate and return temperature in district heating is the biggest issue since, the parameters for heat exchanger and exhaust gases are fixed for designing the condenser (Cuadrado, 2009). The relation of power recovered in FGC and various district heating return temperature and different fuels is provided in Figure 9.

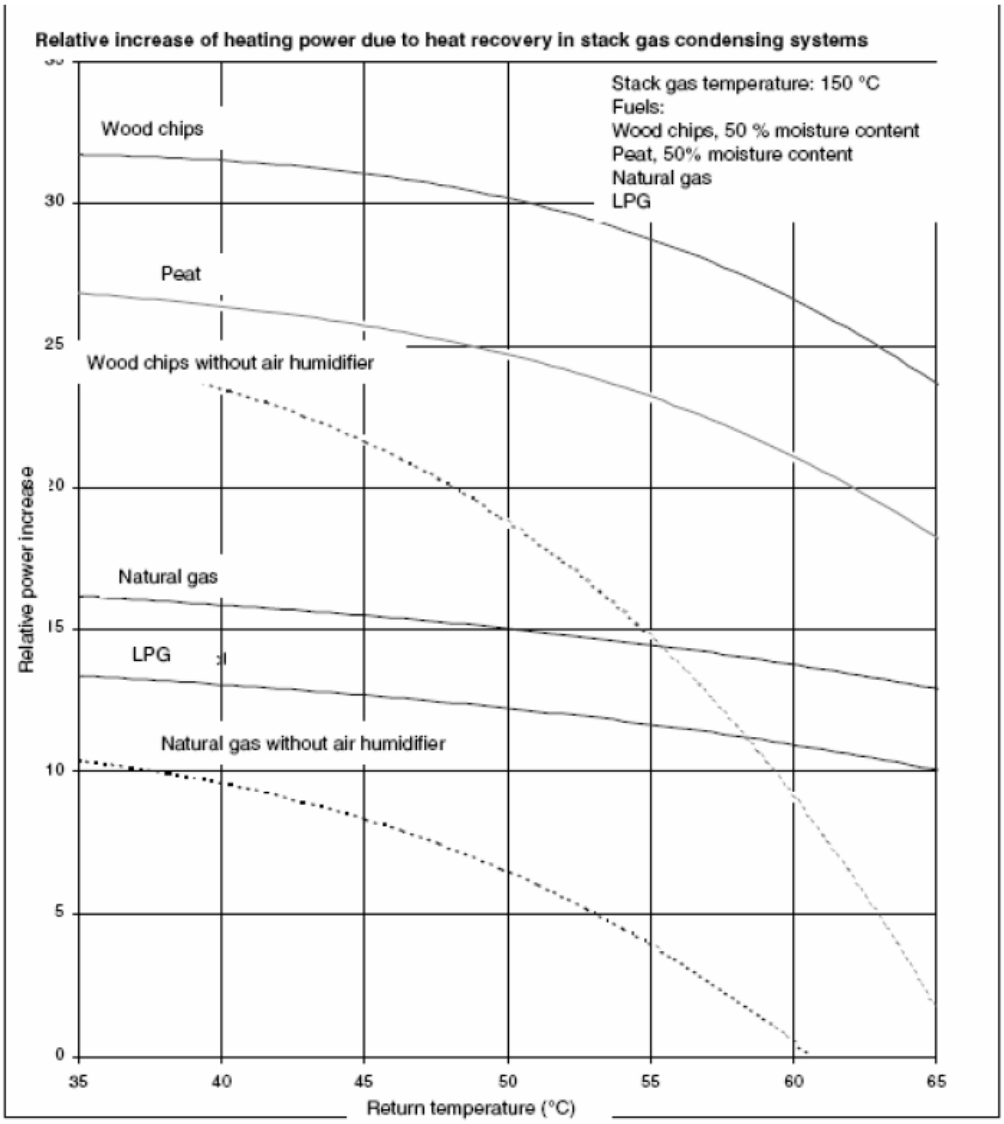

Figure 9. Dependency of power recovered in the flue gas condenser with respect to various district heating return temperature and different fuels (Cuadrado, 2009).

The cooling capacity of flue gas condenser increases by reducing the return temperature that means the amount of condensation of vapor increases which is shown in Figure 9. The extreme values of district heating return temperature that can last for few hours, does not have significant impact on heat recovery (Cuadrado, 2009).

2.5.2 Environmental impacts

Flue gas condenser provides the opportunity of utilizing extra heat from flue gas, increase overall thermal efficiency and reduces the emissions of particulates and gaseous elements to the atmosphere (Singh & Shukla, 2014). Researches have indicated that, FGC installment provides significant reduction of SO_2, HCl emissions and meet the BAT-AELs requirements. However, NO_x emissions reductions are moderate and need alternative solutions such as flue gas recirculation, combustion optimization and optimization of SNCR unit (Hutson, et al., 2008). Another research on flue gas condensing with spray tower has indicated that particulates from flue gas can be reduced by 90% and NO_x by 25% (Selivanovs, et al., 2017).

Flue gas condensation is not limited to condensation of water vapor only, but acids present in flue gas also condensate with respect to their dew points. However, this depends on the characteristics of fuel. Sulphur oxides have higher dew point and are first to condense out (Samuelson, 2008). Condensate sulphur oxides are treated by either by use of Sodium hydroxide (NaOH), Calcium hydroxide ($Ca(OH)_2$) or Calcium carbonate ($CaCO_3$) by maintaining the pH between 5 to 6 (Vehlow & Dalager, 2010).

To further increase the quality of condensate, bag house filter (BHF) are connected after FGC unit. The research on condensate quality from FGC have indicated that the actions such as bag filtration, pH control and condensate cooling are enough to meet the requirement of BAT-AELs for waste water treatment. The FGC also enables to lower the plume rise (Uotila, 2015).

3 SCRUBBER

Scrubbers are emission control equipment installed in the power plants. They are used to remove particulates or gases, especially acid gases from flue gas, and used for moisture recovery from flue gas by condensation. The scrubber can be categorized into two main types before further sub-categorizing: wet scrubbing and dry scrubbing. Wet scrubbing uses scrubbing solution such as water or other reagents, which encounters flue gas by the use of spray nozzle. It is used to clean various gaseous components and dust particles. Whereas, dry scrubbing on other hand uses acid gas sorbent material, which is, dry in nature and does not saturate the flue gas stream. Dry scrubbers are used for removing acidic gases such as SO_2 and HCL and are often used for removal of odorous and corrosive gases in the waste treatment plant (Pence, 2012).

Dry scrubbing is sub-categorized into two groups: dry sorbent injectors (DSIs) and spray dryer absorbers (SDAs). In DSIs, alkaline material is introduced to react with acid gases and can be in injected in different locations such as flue gas duct and combustion chamber. Solid salts are formed after the result of reaction and are removed in particulate control device. SDAs involves the introduction of absorbing tower where, the gas gets contact with atomized alkaline slurry to form solid salts which are also removed in particulate control device. SDAs has the removal efficiency of more than 80% of the acid gas (Pence, 2012).

3.1 Wet Scrubber

Wet scrubber has been widely used to remove acidic gases, particulates and mist from the flue gas with significantly less risk of erosion, fire and explosion and it operates around the dew point of water vapor of the flue gas (Singh & Shukla, 2014). Since, water is used as major scrubbing agent; there is decomposition of salt, which leads to water pollution and foul smell unless treated later (Park, et al., 2005). There are different types of wet scrubbers depending on how the liquid and gas phase are brought into contact such as spray tower, cyclone spray tower, dynamic scrubber, tray towers, orifice scrubber, venturi scrubbers, etc.

Dust particles are removed in wet scrubbers by capturing them in liquid droplets, whereas, gases are either dissolved or absorbed into the liquid. The ability to collect particles by wet scrubber is directly related to its power input. Particles less than five µm are collected by spray towers, which is low energy device. However, for removal of larger, venturi scrubbers are used which in other hand uses high energy and are highly efficient. The advantages of

wet scrubbers such as, ability to handle high temperature and moisture, removal of both gases and particulates and neutralization of corrosive gases makes it a popular choice for emission control in power plants (Pence, 2012).

3.1.1 Spray tower

Spray tower is the low energy consuming flue gas cleaning device with simple design and no internal configuration except spray nozzles Spray towers are used either first or second stage unit for flue gas desulfurization due to their ability to process large volume of corrosive gases. The removal efficiency of spray towers are higher if the gases are very soluble (Pence, 2012). Figure 10 represents the basis configuration of the spray tower scrubber.

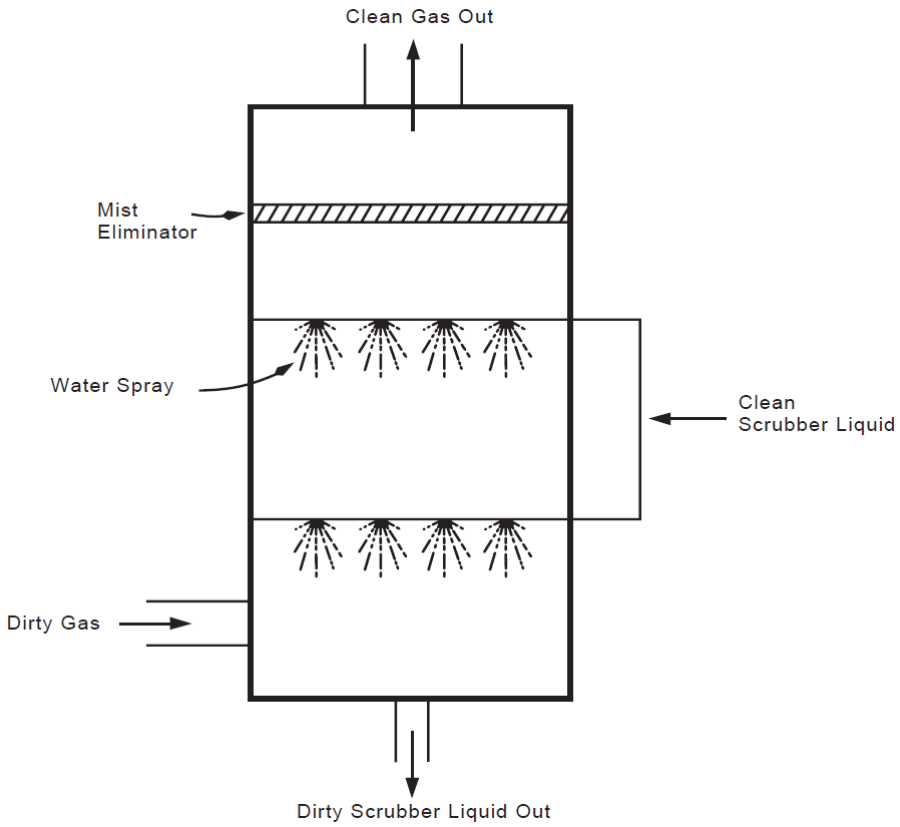

Figure 10. Schematic of spray tower (Wark, et al., 1998)

Spray tower is the simplest type of wet scrubber system and have lower capital costs. Towers can be placed both horizontally and vertically depending upon the gas flows. Water nozzle sprays are mounted either on the wall of the tower or arranged as array in the tower center. Water droplets from nozzles comes to contact with the flue gas through interception and diffusion. Large droplets are then settled at the bottom of the chamber and entrained droplets

in the gas are collected on the mist eliminator (Mussatti & Hemmer, 2002). The operating parameters of spray tower is provided in Table 7.

Table 7. Typical operating parameters of spray tower (Pence, 2012).

Pollutants	Liquid inlet pressure (kPa)	Liquid to gas ratio (l/m^3)	Pressure drop (cm of water)	Removal efficiency
Particlulates and gas	70-2,800	0.07-2.70	1.3-7.6	50-90% for gas 2-8 µm particles

The typical removal efficiency of particles by spray towers depends upon the particles specific sizes. Although the range 2-8 µm diameter is provided in Table 7, the removal efficiency for larger than 5 µm is 90%, 3 to 5 µm is 60 to 80% and particles below 3 µm is less than 50% (Mussatti & Hemmer, 2002).

Cyclone spray tower is usually low to medium pollutant control device where liquid is sprayed inside the tower and inlet gas enters the device tangentially and swirls in corkscrew motion as shown in Figure 11. They are more efficient than spray towers but less efficient than venturi scrubbers. One of the main disadvantage of cyclonic spray towers is that they are unable to remove sub micrometer particulates and are not capable of absorbing most chemical pollutants from flue gas (Pence, 2012).

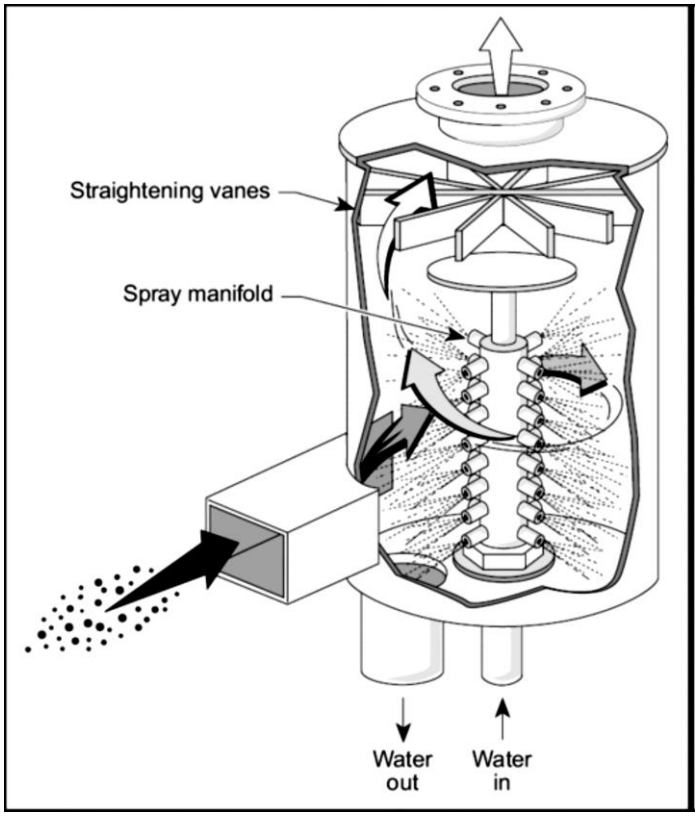

Figure 11. Typical cyclonic spray tower (Pence, 2012).

3.1.2 Venturi scrubber

Venturi scrubbers are expensive scrubber than spray tower and cyclonic spray towers, which has converging-diverging shaped flow chamber. Figure 12 represents the simple schematic of Venturi scrubber. The inlet section is converging which allows to increase the velocity and turbulence of the flue gas. The middle section is called throat where scrubbing liquid is injected and is atomized by the turbulence in the throat. This phenomenon in throat improves the efficiency of gas-liquid contact. The later part is diverging section where gas liquid mixture is diffused causing deceleration and particle-droplet impacts (Mussatti & Hemmer, 2002). There is a short contact time between high inlet gas velocity due to converging and scrubbing liquid, which can result in limitation in gas absorption (Pence, 2012).

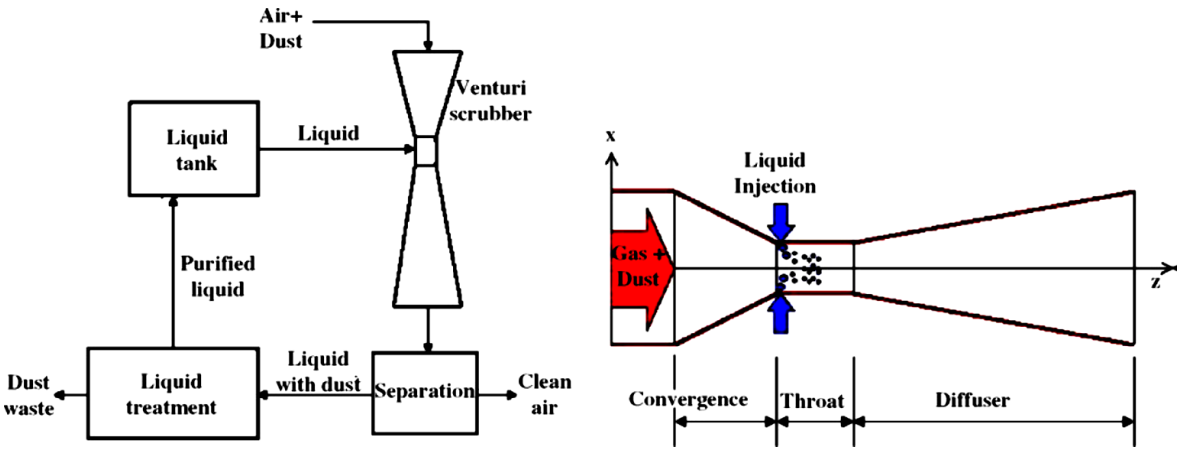

Figure 12. Schematic of Venturi scrubber (Pak & Chang, 2006).

The three-phase flow of liquid, gas and dust are dispersed in Venturi scrubber. The interaction between these phases and atomization of liquid jet have direct impact on the performance of Venturi scrubbers (Pak & Chang, 2006). High turbulence and high gas velocities in the throat and increase in pressure drop results in higher collection and cleaning efficiency of Venturi scrubber (Mussatti & Hemmer, 2002).

Based on liquid injection approach, Venturi scrubbers are classified as wetted throat and non-wetted throat. In Wetted throat venturi scrubbers, liquid is sprayed at the converging section where the liquid coats the venturi throat, which is beneficial for cleaning hot, dry flue gas containing dust. In non-wetted throat venturi, liquid is sprayed at or before the throat where liquid is not coated in throat surface, which makes it beneficial for cleaning cool and moist flue gas (Pence, 2012). Venturi scrubbers with round shaped throat can handle the flue gas flow up to 88,000 m^3/h (Brady & Legatski, 1977). For flow rate larger than this, different Venturi scrubber designs such as rectangular, long, narrow, etc. throats are used (Pence, 2012).

Venturi scrubbers are beneficial if scaling a scrubber is a problem, high concentration of dust in inlet flue gas, presence of sticky dust and if the gas is chemically reactive with the liquid. Lower gas velocities and higher liquid to gas ratio maximize the absorption of gases in Venturi scrubbers. For maximization of flue gas absorption, liquid to gas ratio is approximately 2.7 to 5.3 l/m^3 (Pence, 2012). The gas and particles removing characteristics of Venturi scrubbers is shown in Table 8.

Table 8. Gas and particles removing characteristics of Venturi scrubber (Pence, 2012) (Pak & Chang, 2006).

Pollutant	Liquid inlet pressure (kPa)	Liquid to gas ratio (l/m^3)	Pressure drop (cm of water)	Removal efficiency
Particles	< 7-100	0.67-1.34	50-250	0.5-10 µm
Gas		2.7-5.3	13-250	30-60%

The high particle collection efficiency of venturi scrubbers is resulted from the high velocities and turbulence of the gases in the throat. The removal efficiency of particle of diameter larger than one µm is 70-99% whereas less than 1 µm is greater than 50% (Mussatti & Hemmer, 2002).

3.2 Design parameters for wet scrubbers

Six main parameters should be considered when designing the wet scrubbers for the flue gas. They are: 1) Particle size distribution and loading, 2) gas velocity and its pressure drop, 3) waste gas flow rate, temperature and humidity, 4) droplet size, 5) liquid to gas ratio, 6) residence time (Mussatti & Hemmer, 2002). In order to ensure the evaporation, the spraying water temperature should be greater than dew point of the gas (Veidenbergs, et al., 2010).

The size distribution of particulates have impact on the performance of the wet scrubbers. Particle size less than 0.1 µm diameter are removed through diffusion process. The PM loading is the mass of PM per unit volume at the scrubber inlet. The PM loading affects the liquid to gas ratio but also the solid content in recycled scrubbing liquid. If the loading of particulates increases, the liquid to gas ratio also should increase to have same collection efficiency and more volume of clean scrubbing liquid should be added to have same solid content in the recycled liquid (Mussatti & Hemmer, 2002).

The gas velocity and pressure drop play vital roles in particles collection efficiency. If the relative velocity of gas and liquid droplets are increased, smaller particles are collected. Pressure drop should be maintained across the scrubbers and increasing pressure drop does not imply higher collection efficiency. Diversion section in venturi scrubbers are designed to lower gas speed, low turbulent losses and for high amount of energy recovery (Mussatti & Hemmer, 2002). It should be noted that, when relative velocities are increased, it increases the energy demand, pressure drop and operation cost of the scrubber (Cooper & Alley, 1994).

The flow rate of the flue gas is the most vital parameter for designing wet scrubber. If the flow rate of flue gas is higher, larger scrubbing system and liquid is required and vice versa. The inlet temperature and humidity determines the amount of evaporation in the scrubber system. The droplet size has direct impact of particulates collection and is determined by nozzle type in spray towers and liquid to gas ratio and gas velocity in the case of venturi. Due to the large surface area to volume ratio, small water droplets are able to capture more particles per volume of liquid that is injected (Mussatti & Hemmer, 2002).

The ratio of liquid to gas is increased to have higher collection efficiency. On the other hand, increasing the ratio also increases the amount of scrubbing liquid, pump power and hence operating costs. Residence time is the contact time between liquid and gas, which can be increased, for example in venturi by increasing the length of throat and diverging section. When the residence time is increased, contact between suspended particulates and liquid increases which increases the collection efficiency (Mussatti & Hemmer, 2002).

4 HEAT RECOVERY CONNECTION TYPES

There are various ways of heat recovery connection. The heat can be recovered using either heat pump, combustion air humidification or heat exchangers. The heat can be directly used by applying it to increase the return temperature of district heating. Figure 13 provides graphical representation of plain condensation of flue gas moisture in condensing scrubber. In this process, the water vapor in the flue gas is lowered to dew point and is condensed either in condenser surface or to water circulation. Heat released during condensation process is transferred to district heat water. The resulted condensate is acidic and Sodium Hydroxide (NaOH) is used for neutralization (Veidenbergs, et al., 2010).

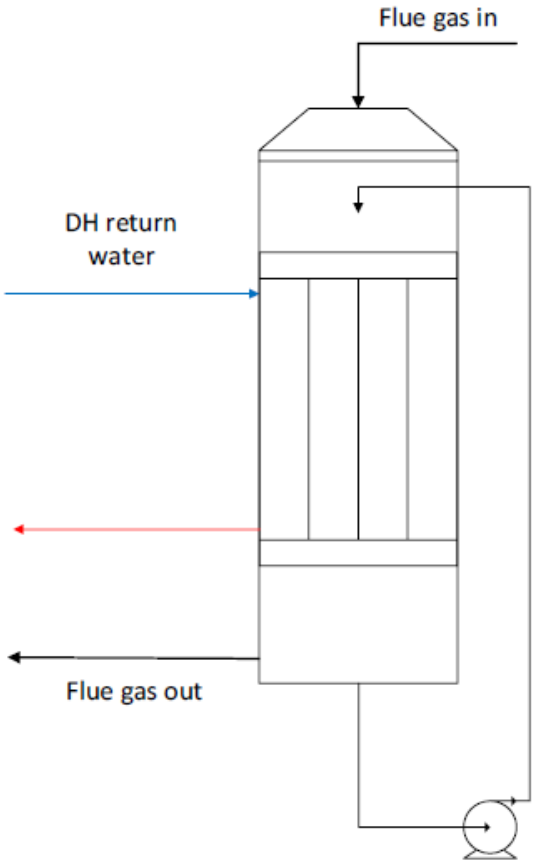

Figure 13. Schematic of plain condensation of flue gas moisture in a tube-condensing scrubber (Uotila, 2015).

Another method to increase the heat recovery in FGC is the addition of combustion air humidifier. The schematic layout of CAH and FGC unit is shown in Figure 14. The configuration of CAH includes packed bed where flue gas in fed from bottom where it is

humidified with water sprayed from the top. The main purpose of addition of CAH is to increase the moisture content of flue gas and combustion air. The increase in moisture content in flue gas also increases the dew point of moisture in flue gas. Consequently, the condensation of flue gas could be achieved at higher temperature and increases the heat recovered in FGC (Zhelev & Semkov, 2004). The CAH method is more efficient when return temperature of district heating water is high (Uotila, 2015).

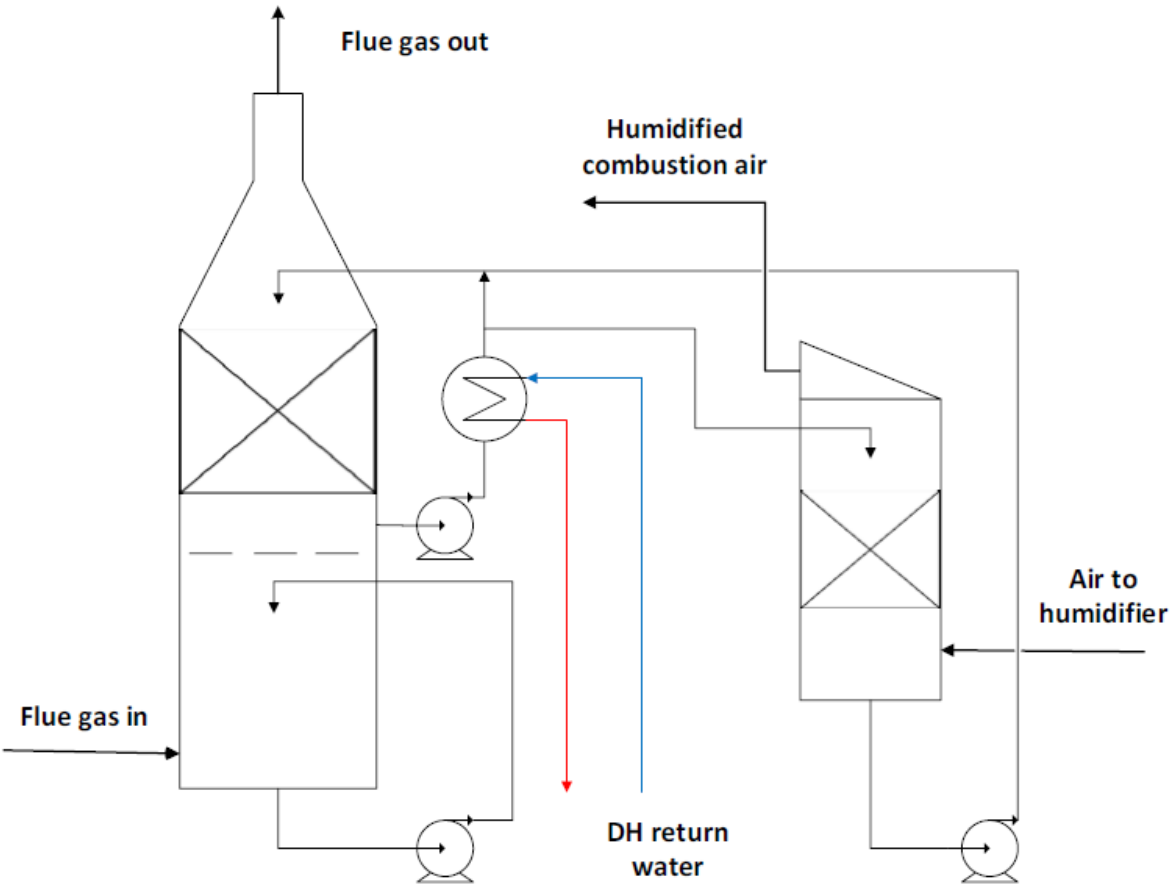

Figure 14. Schematic of heat recovery by the addition of combustion air humidifier into FGC unit (Uotila, 2015; Zhelev & Semkov, 2004).

The method studied in detail in this thesis paper is the integration of heat pump in FGC unit for heat recovery. Figure 15 represents schematic of heat recovery connection with heat pump. Heat transfer is obtained through direct contact between liquid and flue gas in spray tower. The two stage scrubbing is used where; lower scrubber is used for removal of sulphur dioxide (SO_2) and upper scrubber for heat recovery (Teppler, et al., 2017). Heat pump is used for cooling of DH return water to increase the condensing efficiency in FGC. Water

recovery in this kind of connection was greater than 80% and is suitable for fuels with high moisture content (Han, et al., 2017).

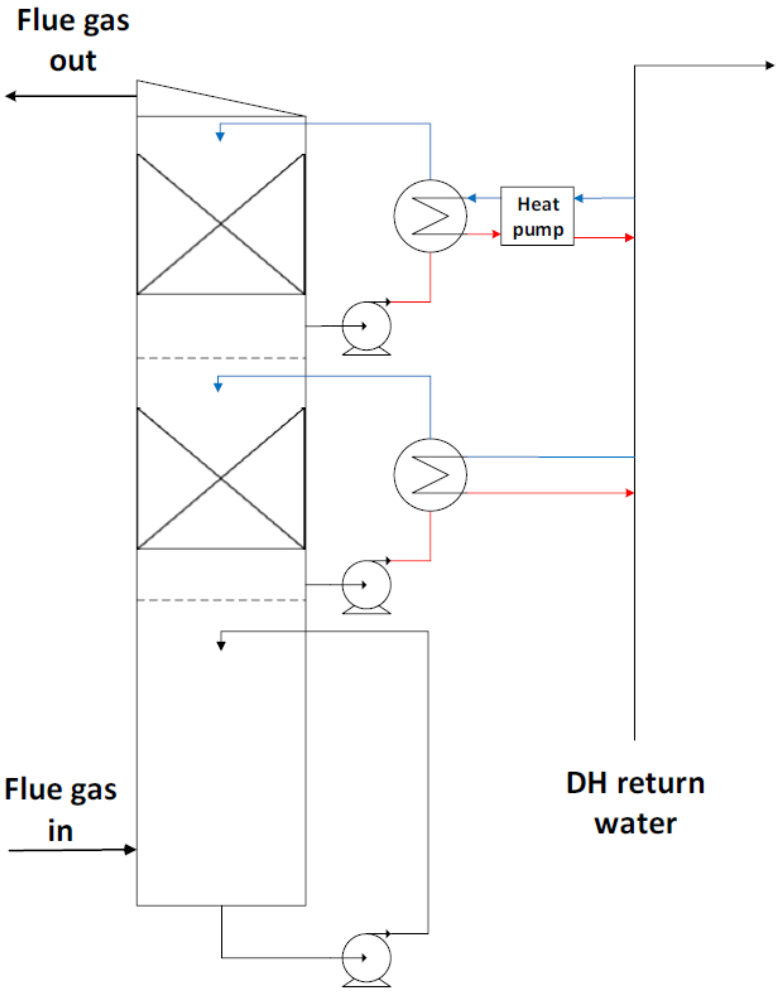

Figure 15. Schematic of heat recovery connection with heat pump (Uotila, 2015; GÖTAVERKEN MILJÖ, 2014).

The heat pump connection is powered by either steam or electricity, which in result lower the production of electricity by power plant. To be cost-efficient and energy efficient for heat pump, the return temperature of district heat network must be above 50°C (Axby & Pettersson, 2004).

4.1 Heat pump

Heat pump is a device that uses external source of energy to pump heat from lower temperature body to higher temperature sink. It uses refrigerant as a working fluid that undergoes vapor-compression refrigeration cycle, which is shown in Figure 16. During

vapor-compression cycle, the refrigerant gains energy in the low temperature and pressure evaporator and it transfers heat to the high temperature and pressure condenser due to the work done in the compressor (Borgnakke & Sonntag, 2012).

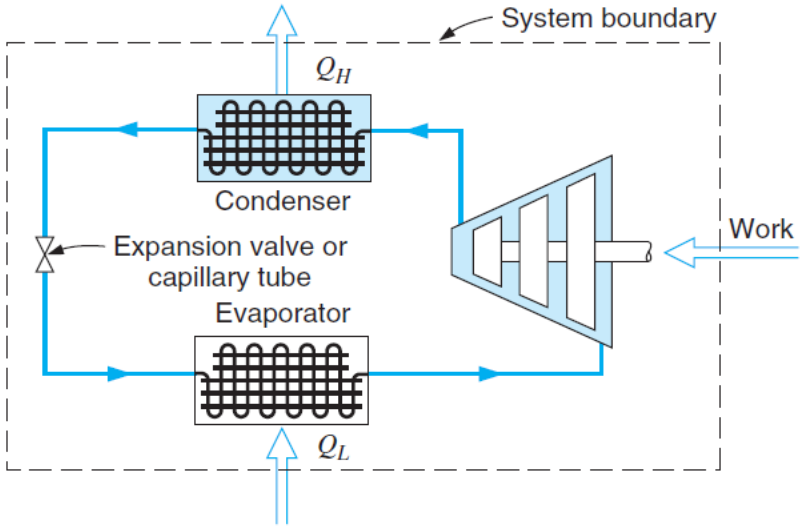

Figure 16. Schematic of vapor-compression refrigeration cycle (Borgnakke & Sonntag, 2012).

During vapor-compression cycle, liquid state refrigerant, which has low pressure and temperature gains heat in the evaporator causing it to evaporate. The refrigerant then passes through compressor where it gains pressure and as consequence, it gains temperature. The higher temperature refrigerant releases heat in the condenser causing it to condensate. The expansion valve is then used to expand the working fluid before it returns to the evaporator (Borgnakke & Sonntag, 2012). Based on operating mode, heat pumps are classified as mechanical driven heat pumps (consuming electricity) and absorption heat pumps (using heat from hot water or flue gas). Mechanical driven heat pumps are more efficient than absorption heat pumps (Garcia, et al., 2012).

Based on heat transfer medium, heat pump can be classified into mainly four groups: air-to-air, air to water, water to water and water to air. Air to air heat pumps are widely used for air conditioning in buildings and the process can be reversible for heating purpose. Air to water heat pumps provide can provide both space heating and hot water, and it avoid the expensive water loops. Water to water heat pumps uses available water sources for both heat source and sink, and has higher value of COP than air to water heat pumps (IEA, 2011).

4.1.1 Coefficient of performance (COP)

The efficiency of heat pump is expressed as coefficient of performance (COP). It is expressed as ratio of heat released to higher temperature body to the work done by the pump. The energy balance and expression for COP of heat pump is provided in equations (4), (5), and (6) (Borgnakke & Sonntag, 2012).

$$Q_L + W_{in} = Q_H \tag{4}$$

$$COP = \frac{Q_H}{W_{in}} \tag{5}$$

$$W_{in} = \frac{Q_L}{COP - 1} \tag{6}$$

Where,

W_{in} = Work done by pump (W)
Q_L = Heat absorbed by refrigerant from lower temperature body (W)
Q_H = Heat rejected by refrigerant to higher temperature body (W)

The typical COP for ground source heat pump is 2.5 to 6, air source heat pump is 2 to 5 and reversible air-to-air heat pump is 2 to 6 (IEA, 2011). The research conducted by (David, et al., 2017) for large-scale electric heat pumps in district heating systems estimated the average COP of 4.5 for output temperature of below 70^{o}C, 3.6 for 71-80^{o}C and 3.7 for above 80^{o}C for existing large heat pumps in EU district heating systems. Figure 17 shows the COP value of water-to-water heat pump as a function of exit temperature of heat source and sink.

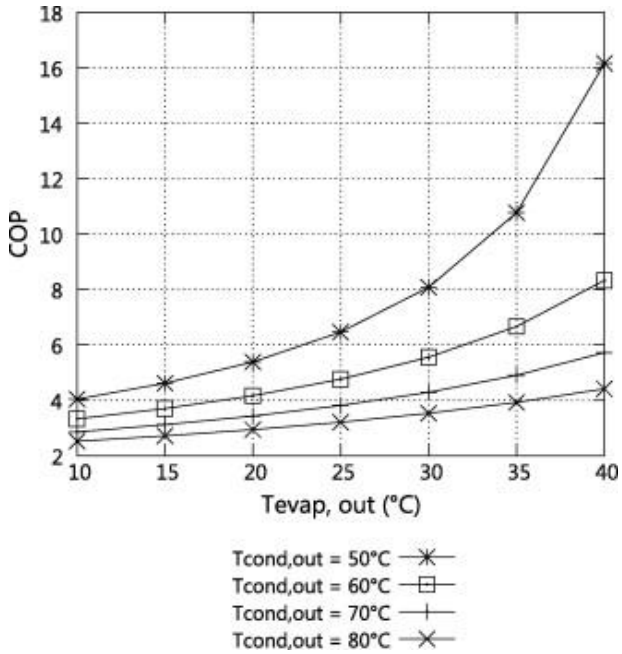

Figure 17. COP value for water-to-water heat pumps depending on exit temperatures of heat sink and source (Tassou, 1988).

The COP of heat pump is higher when the temperature difference is smaller and vice-versa. As temperature exiting heat source decreases, the COP value also decreases. However, highest COP can be achieved if inlet temperature for evaporator is fixed and mass flow is increased which results in increase in outlet temperature from evaporator.

4.1.2 Heat pump integration in district heating

District heating uses mostly excess heat sources from industrial processes, CHP plants and waste to energy plants but during recent decade's renewable heat sources such as biomass fuels, solar energy and geothermal energy has been on rise. The main heat users are industries, residential buildings, service sectors, etc. and 85% of total heat deliveries account to Russia, China and EU states (IEA, 2016).

In district heating (DH) network, heat pump utilizes waste heat to increase the energy of lower temperature network to higher temperature network and consequently increasing energy efficiency and decarbonization of energy sector. The major heat sources for large-scale heat pumps in district heating networks are sewage water, ambient water (sea, lake or river water), industrial waste heat, geothermal water, flue gas and solar heat storage. The existing temperature range at the heat source for utilizing flue gas heat is between 34 and 60^{o}C (David, et al., 2017). The share of large heat pump in DH in Nordic countries is provided in Figure 18.

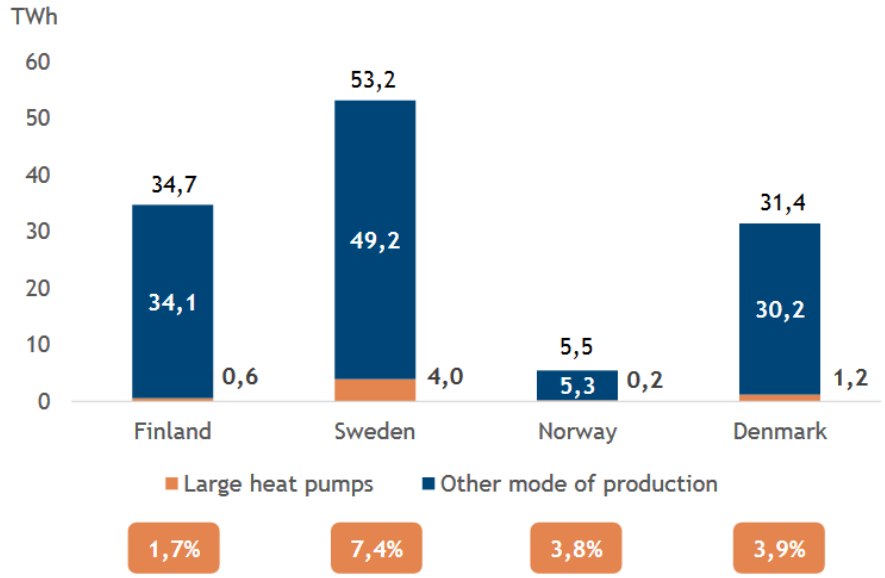

Figure 18. Share of large heat pumps in district heating production in Nordic states (Passi, et al., 2016).

The average COP value for heat pumps in existing DH networks is between 3 and 4 in European states. However, two heat pumps in Sweden have achieved the highest COP of 6.5 by using R-134a refrigerant and heat pump in Denmark have achieved COP of 6.3 by using NH_3 refrigerant (David, et al., 2017).

The integration of heat pump in DH is beneficial for reducing emissions from energy sector by limiting energy and heat losses. Heat pumps have almost zero or near-zero emissions when renewable heat source is used (Sayegh, et al., 2018). The relative emission changes in district heating due to the integration of heat pump of seasonal performance factor (SPF) of 4 in Sweden is provided in Figure 19.

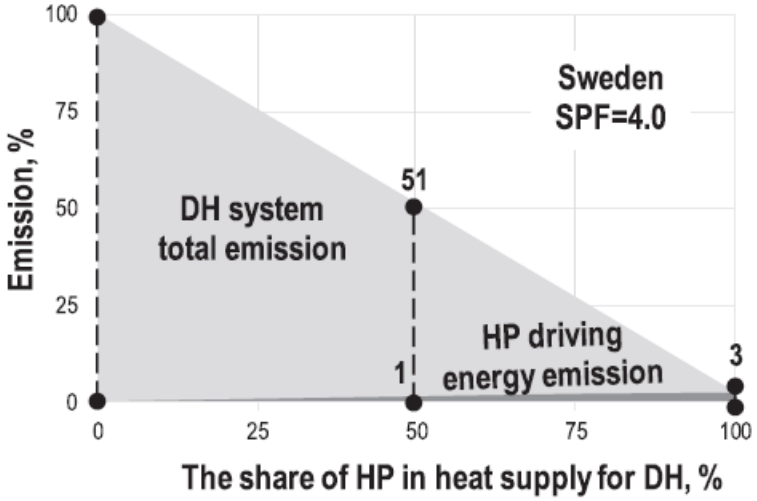

Figure 19. Relative emission changes in district heating due to the integration of heat pump of seasonal performance factor (SPF) of four in Sweden (Sayegh, et al., 2018).

The results in Figure 19 accounts the power generation technologies, emissions from national grid of Sweden and share of renewables in electricity production. It shows that, 50% integration of heat pumps in DH network contribute to emission reduction to 51% and 100% integration contribute to reduction of 3%. Different factors such as fuel source, technical characteristics and emissions should be taken into account when integrating heat pump in DH network and the promotion of cogeneration plants based on renewable fuels and low-carbon technologies enables sustainable integration of heat pump (Sayegh, et al., 2018).

5 MODEL DEVELOPMENT

5.1 IPSEpro Software

IPSEpro is a software designed by SimTech for heat balances and simulating process for various applications such as thermal power, biomass gasification, desalination, flue gas cleaning, etc. Each component is modelled and designed in IPSEpro and can be connected to make complete life cycle of process plant. Figure 20 represents the working principles of IPSE software.

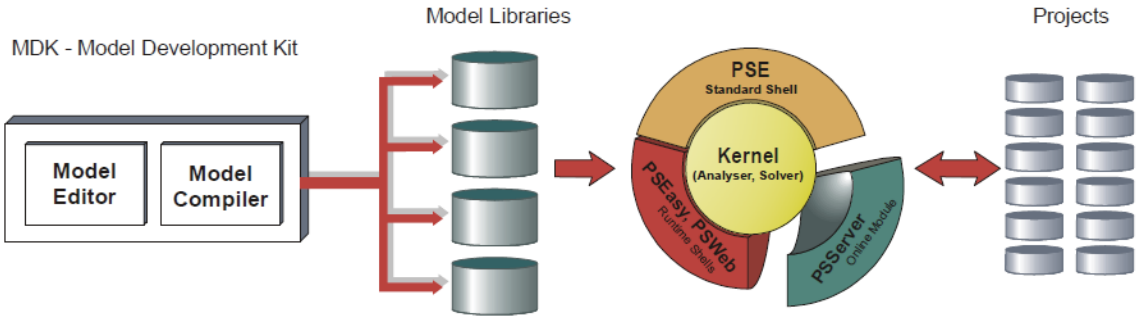

Figure 20. Working structure of IPSEpro (Courtesy: http://www.simtechnology.com)

In IPSEpro, three different types of models are defined: Units, Connections and Globals and have triangular relation between them. Units represent the actual equipment such as pipe, turbine, boiler, etc. and are nodes in process network. Connections allow units to transfer information or fluid between each other. For example, stream is a connection, which is shown in Figure 21. On the other hand, globals represent the information, which can be used undefined number of streams or objects. For example, composition, which can be water or chemical, can possibly share by many streams.

5.1.1 Model Development Kit (MDK)

MDK is a component level system in IPSEpro where models are designed both mathematically and graphically. In addition, existing model libraries can also be modified by using MDK. MDK consists of two functional units: Model editor and Model Compiler. Model editor provides platform to write mathematical equations to develop model and allows designing icons that represent the model. On the other hand, model compiler translates the equations provided to form model in model editor in binary form.

The equation provided in MDK is straightforward and the equations can have conditional statements and other sub-equations. If the two numerical expressions have equal values, a valid solution is found. The language representing components model mathematically in MDK is called Model Description Language (MDL), which is equation-oriented language. Although, the traditional programming language such as C has sequential concept, MDL does not possess such concept, and equation sequences have no effect on the how the equation are processed.

5.1.2 Process Simulation Environment (PSE)

PSE is the process level component of the IPSEpro. With PSE, process model are created by using the components from the existing library. It provides graphical user interface and freedom to choose in arranging the available components and assigning the data independently. Arranging components implies satisfying the all the equations and variables of each component into single system of equation. The flowsheet is used to input all the data related to the process model. Figure 21 provides the information how the components are connected in the PSE and the theory behind the connections.

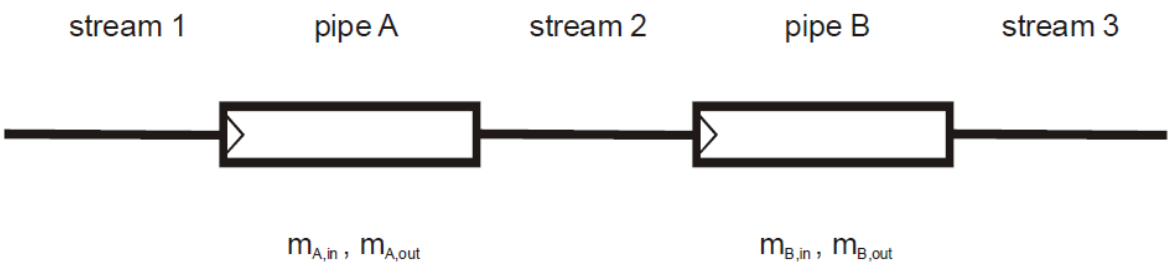

Figure 21. Basic theory of connected components in PSE (Courtesy: http://www.simtechnology.com)

Two pipes A and B are connected with mass flow rate in stream 1, 2 and 3 in Figure 21. In order to satisfy the continuity principle, mass flow rates for in and out of the pipe must be same as provided in equation (7) and (8).

$$m_{A,in} = m_{A,out} \tag{7}$$

$$m_{B,in} = m_{B\,,out} \tag{8}$$

The two-phase approach is adopted by PSE to solve the model equations: System analysis and Numerical analysis. In system analysis phase, the optimum solution method, order of

treatment of variables and combining equations if need is carried out. In numerical analysis phase, PSE solves the equations that are predefined in analysis phase.

5.2 Modeling methodology

5.2.1 Flue gas composition and enthalpy

The composition of flue gas and its enthalpy is directly dependent on fuel composition and excess air used in boiler. The fuel composition is fixed in boiler model. The Table 9 list all the chemicals with temperature and pressure range in IPSEpro at which different properties can be extracted for calculation.

Table 9. List of chemicals components, which are available in IPSEpro database. (Source: SimTech)

Variable	Component	Temperature [°C]		Pressure [bar]	
		min	max	min	max
AR	Argon	-30.0	5726.85	0.1e-6	20.0
C2H6	Ethane	-30.0	5726.85	0.1e-6	35.0
C3H8	Propane	-25.0	5726.85	0.1e-6	35.0
CH4	Methane	-30.0	5726.85	0.1e-6	35.0
CO	Carbon monoxide	-30.0	5726.85	0.1e-6	100.0
CO2	Carbon dioxide	-30.0	5726.85	0.1e-6	35.0
H2	Hydrogen	-30.0	5726.85	0.1e-6	35.0
H2O	Steam (as ideal gas)	-30.0	5726.85	0.1e-6	30.0
H2S	Hydrogen sulfide	-20.0	5726.85	0.1e-6	100.0
N2	Nitrogen	-30.0	5726.85	0.1e-6	35.0
O2	Oxygen	-30.0	5726.85	0.1e-6	35.0
SO2	Sulfur dioxide	0.0	5726.85	0.1e-6	10.0

The difference of flue gas enthalpy at different temperatures of inlet ant outlet of FGC is the key way to calculate the heat recovered. First, molar flow of flue gas is estimated from the gas composition induced by the excess air in boiler and is provided in equation (9).

$$g = \sum \left(\frac{y_i}{MW_i} \right) \quad (9)$$

Where,

g = molar flow of flue gas [moles/g]
y_i = mass fraction of individual flue gas component [-]
MW_i = molecular weight of individual flue gas components [g/mol]

The estimation of enthalpy in IPSEpro based on pressure-temperature and pressure-steam fraction are provided as follows.

Enthalpy = FG.Composition.fhpt(p,t)

Enthalpy = Water.Composition.fhpx(p,x) where, $[0 \leq x \leq 1]$

5.2.2 Partial pressure

The calculation of partial pressure of the water vapor in the flue gas is needed to estimate the recovery of both latent heat due to condensation and sensible heat. At dew point temperature, the air is saturated with water. If it is cooled below that temperature, condensate starts to occur. The dew point of moisture is dependent to its partial pressure in the flue gas.

The partial pressure of water vapor in the flue gas (p_m) is determined by using equation (10).

$$p_{in} = \frac{P_{in} * \frac{y_{H_2O}}{MW_{H_2O}}}{g} \quad (10)$$

Where,

P_{in} = total pressure of the flue gas at the inlet [bar]
p_{in} = partial pressure of the water vapor in flue gas inlet [bar]
y_{H_2O} = mass fraction of water vapor in flue gas [-]
MW_{H_2O} = molecular weight of water [g/mol]

Since, the flue gas exiting the heat exchanger is assumed saturated as condensed water, the partial pressure of water vapor exiting flue gas is determined by using equation (11).

$$p_{out} = \frac{P_{out} * \frac{y_{H_2O}}{MW_{H_2O}}}{g} \quad (11)$$

5.2.3 District heating water

The recovered heat from FGC is utilized for heating the incoming water from district heating network. The energy balance of district heating water is provided in equation (12) which is calculated by heat transfer from hot side source to cold water.

$$m_{dh} * \left(h_{dh_{out}} - h_{dh_{in}}\right) = m_{hot} * \left(h_{hot_{in}} - h_{hot_{out}}\right) \quad (12)$$

Where,

m_{dh} = mass flow rate of district heating water [kg/s]
m_{hot} = mass flow rate of hot side water [kg/s]
$h_{dh_{in}}$ = enthalpy of district heating inlet water [J/kg]
$h_{dh_{out}}$ = enthalpy of district heating outlet water [J/kg]
$h_{hot_{in}}$ = enthalpy of inlet hot water [J/kg]
$h_{hot_{out}}$ = enthalpy of outlet hot water [J/kg]

5.2.4 Log mean temperature difference (LMTD)

LMTD is used to determine the overall heat transfer rate and heat transfer area of a heat exchangers. It is determined by the equation provided in equation (13).

$$Q = U * A * \Delta T_{lm} \quad (13)$$

Where,

Q = Heat transferred [W]
U = Overall heat transfer coefficients [W/m^{2}K]
A = Heat transfer area [m^2]
ΔT_{lm} = log mean temperature difference [^{o}C]

The calculation of LMTD depends upon the direction of flow of fluid in heat exchanger. The fluid flow in heat exchanger for district heating network is taken as counter-flow. The working principle of counter-flow heat exchanger is provided in Figure 22. The x in the figure denotes the location point, where point 1 is inlet of hot side and point 2 is inlet for cold side.

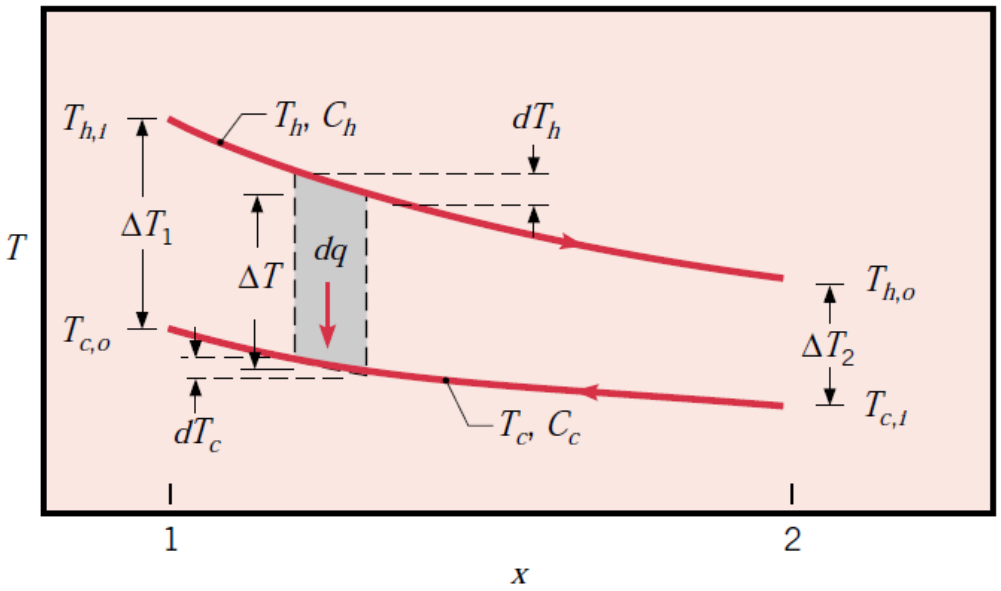

Figure 22. Principle of Counter flow heat exchangers (Incropera, et al., 2007).

Based on Figure 22, the equation of log mean temperature difference for counter-flow heat exchanger is provided equation (14).

$$\Delta T_{lm} = \frac{\Delta T_2 - \Delta T_1}{\ln\left(\frac{\Delta T_2}{\Delta T_1}\right)} \tag{14}$$

Temperature differences are defined in equation (15) and (16).

$$\Delta T_1 = T_{h,i} - T_{c,o} \tag{15}$$

$$\Delta T_2 = T_{h,o} - T_{c,i} \tag{16}$$

Where,

$T_{h,i}$ = Inlet temperature from hot side [°C]
$T_{h,o}$ = Outlet temperature from hot side [°C]
$T_{c,i}$ = Inlet temperature from cold side [°C]
$T_{c,o}$ = Outlet temperature from cold side [°C]

5.3 CHP plant model and parameters

The CHP model used in this thesis paper is based on design model. This plant was modeled at full load with IPSEpro software based on real-time operating performance (Saari, et al., 2016). The fuel used in the model was wood chips with 55% moisture. The chemical composition of wood chips fuel is provided in Table 10.

Table 10. Composition of wood chips fuel.

Wood chips properties	Weight fraction (kg/kg)
C	0.2295
H	0.0251
N	0.0018
O	0.189
S	0.0004
H_2O	0.55
Ash	0.0045

The operation parameters for CHP plant is provided in Table 11. The excess air of 1.19 has been estimated for combustion of biomass fuel and the fuel mass flow of 4.489 has been estimated for the operation of the CHP plant. The losses has been estimated for the boiler. The losses consists of stack loss of 2.91 MW, ash loss of 20.6 kW, carbon loss of 229.6 kW, heat loss of 330 kW, blowdown loss of 146 kW and other losses of 333.6 kW.

Table 11. Operation parameters of the CHP plant.

Nominal fuel power	33.36 MW_{th}
Net electricity generation	8.11 MW_{el}
District heat production	20.00 MW_{th}
Boiler efficiency (LHV)	86.5 %
District heat production efficiency (LHV)	59.9 %
Total efficiency (LHV)	84.2 %

The schematic layout of CHP plant in IPSEpro is provided in Figure 23. The live steam exiting the boiler is further heated in superheater (SH) passes through turbine labeled ‘Reg’ where mass flow rate of steam is controlled. The steam is then extracted though back pressure turbines (labeled T1-T4). The high pressure and temperature steam extracted from the turbine is applied for further CHP process. District heating water is heated by high pressure and temperature steam extracted from turbine (T4) and splitter after SH. It is also applied for heating air by the use of steam condensing air heater (SCAH).

The flue gas exiting BFB boiler is first introduced in SH to increase live steam temperature. In second stage, it is used to heat the feed water in economizer (Eco). The flue gas is then applied to counter heat exchanger (htex counter) to further increase the temperature of feed air. The exhaust gas has temperature of approximately 158^{o}C and moisture content is estimated approximately 18.9% in IPSEpro before leaving to emission control systems.

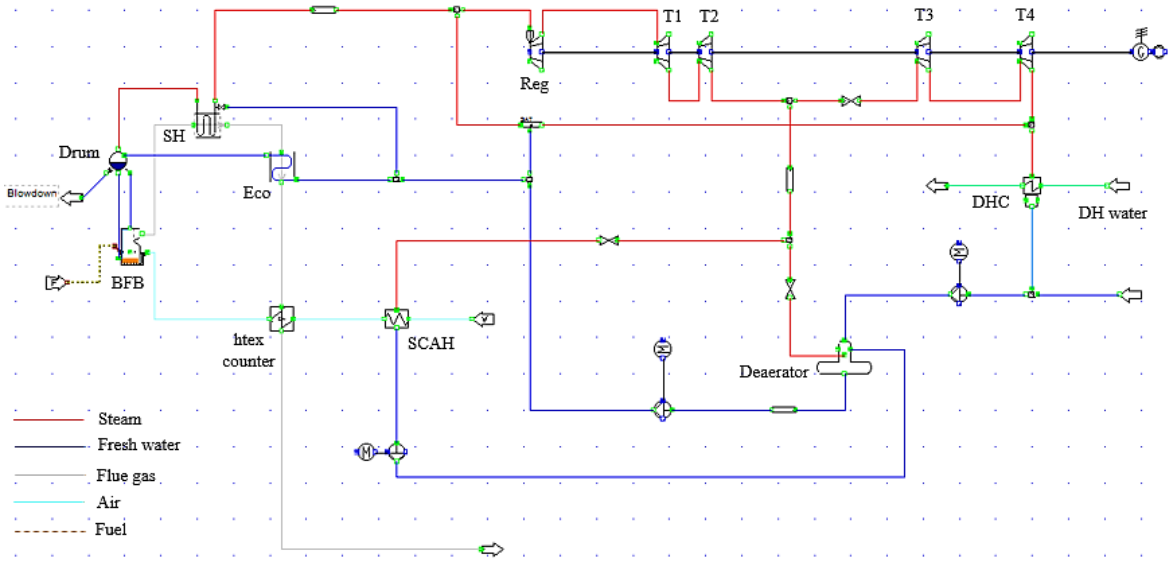

Figure 23. Schematic layout of stand-alone CHP plant configuration in IPSEpro.

5.3.1 Heat pump design

The heat pump is designed to extract the flue gas condensing energy to increase the temperature at the inlet of district heating water. Before integrating the heat pump into the spray tower model, different COP value has been tested with constant mass flow rate by using design CHP model. The different COP of heat pump, temperature at outlet of evaporator and condenser of heat pump is shown in Figure 24.

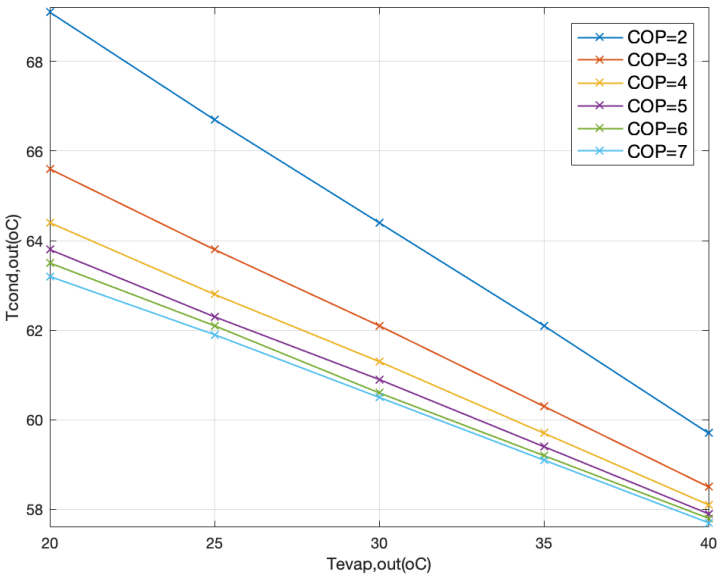

Figure 24. Performance of modeled heat pump in IPSEpro.

5.4 Flue gas condenser model

5.4.1 Basic model (Plain condensation)

The basic model of flue gas condenser provided in Figure 25 works as counter-flow heat exchanger where red line indicates the flow of flue gas and blue line indicates the flow of cold water. It works as a tube condenser, where cold water flow through the tube and flue gas gets contact with tube transferring heat to the cold water. The water vapor in inlet flue gas is condensed due to the heat transfer between hot flue gas side and cold-water side.

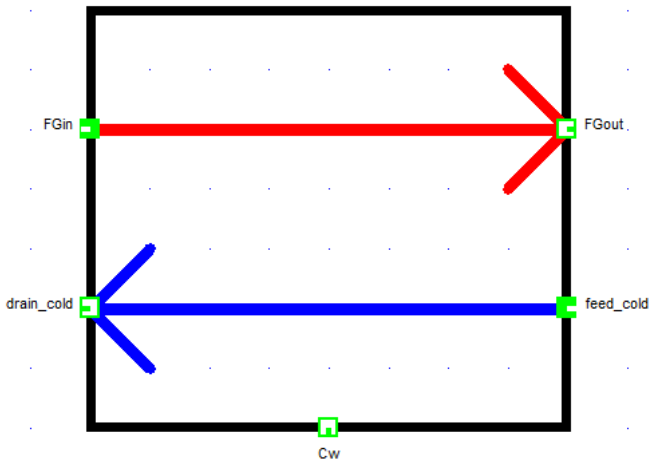

Figure 25. Basic model of FGC (only condensation of water vapor in flue gas)

The mass flow of flue gas decreases at the heat exchanger exit due to the partial condensation of water vapor. The heat energy due to condensation of water vapor of flue gas (both sensible and latent heat) is transferred to water. The mass balances in the FGC heat exchanger are provided in equations (17) and (18).

$$\dot{m}_{FGin} = \dot{m}_{FGout} + \dot{m}_{Cw} \tag{17}$$

$$\dot{m}_{feed\_cold} = \dot{m}_{drain\_cold} \tag{18}$$

Energy balances for FGC are provided in equation (19) and (20).

$$\dot{m}_{FGin} * h_{FGin} - \dot{m}_{FGout} * h_{FGout} - \left(\dot{m}_{Cw} * \left(h_{Cw}(p_{in}, 0) - h_{Cw}(p_{in}, T_{FGin})\right)\right) = q_{trans} \tag{19}$$

$$\dot{m}_{drain\_cold} * h_{drain_{cold}} - \dot{m}_{feed_{cold}} * h_{feed_{cold}} = q_{trans} \tag{20}$$

Where, $\dot{m}$ and h are the respective mass flow rates (kg/s) and enthalpies (J/kg) of flue gas inflow (FGin), flue gas outflow (FGout), cold water inflow (feed_cold), cold water outflow (drain_cold), and condensed water (Cw). The enthalpy $h_{Cw}(p_{in}, 0)$ is enthalpy of condensed water at water vapor partial pressure and saturated water condition. The enthalpy $h_{Cw}(p_{in}, T_{FGin})$ is the enthalpy of moisture at inlet water vapor partial pressure and inlet temperature of flue gas. The difference between these two enthalpy results in enthalpy due to sensible and latent heat. The heat transfer between flue gas and cold side is denoted by q_{trans} (Watts).

5.4.2 Spray tower model

The spray tower model is built to lower the exit temperature of flue gas and increase the return water temperature of district heating network. The working principle of spray tower model is the direct contact between scrubbing water and flue gas. The graphical representation of spray tower model is provided in Figure 26. The model consists of two spray towers: lower spray water (sw1) and upper spray water (sw2), inflow of flue gas (fg_in), outflow of flue gas (fg_out), and flow of drain water as result of condensation of water vapor in flue gas and mass flow of both spray water.

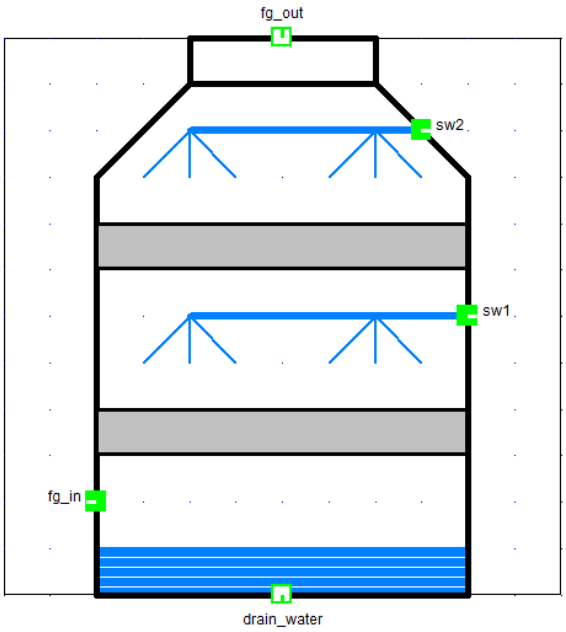

Figure 26. Graphical representation of spray tower model in IPSEpro.

The partial pressure of water vapor in flue gas exiting FGC is assumed saturated and is equal to its saturation pressure. Therefore, the exiting temperature of flue gas is calculated based on saturated water vapor pressure. The two-spray tower model enables the higher amount of

water condensation from flue gas and lower exit temperature of flue gas. The mass balance for spray tower model is provided in equation (21).

$$\dot{m}_{drain\_water} = \dot{m}_{sw1} + \dot{m}_{sw2} + \left(\dot{m}_{fg\_in} - \dot{m}_{fg\_out}\right) \tag{21}$$

The difference of inlet and outlet energy of flue gas, sum of energy flows from two spray towers and addition of sensible and latent heat due to condensation of moisture provides the total energy in condensation tank. The energy balance for spray tower model is provided in equation (22).

$$\begin{aligned} \dot{m}_{fg\_in} * h_{fg_{in}} - \dot{m}_{fg_{out}} * h_{fg_{out}} \\ + \Big(\left(\dot{m}_{fg_{in}} - \dot{m}_{fg_{out}}\right) \\ * \left(h_{drain\_water}(p_{in}, T_{fg\_in}) - h_{drain\_water}(p_{in}, 0)\right)\Big) + \dot{m}_{sw1} \\ * h_{sw1} + \dot{m}_{sw2} * h_{sw2} = \dot{m}_{drain\_water} * h_{drain\_water} \end{aligned} \tag{22}$$

The temperature difference (dt) is defined from the difference between exit temperature of flue gas and water temperature of upper scrubber as provided in equation (23).

$$dt = T_{fg_{out}} - T_{sw2} \tag{23}$$

The mass balance for water vapor in FGC is calculated by the difference of condensate in tank accounting mass flow of both spray tower and water vapor in flue gas exit as provided in equation (24).

$$\begin{aligned} \left(\dot{m}_{fg\_in} * H_20_{fg_{in}}\right) - \left(\dot{m}_{fg_{out}} * H_20_{fg_{out}}\right) - \left(\dot{m}_{drain_{water}} - (\dot{m}_{sw1} + \dot{m}_{sw2})\right) \\ = 0 \end{aligned} \tag{24}$$

6 RESULTS

6.1 Basic model

The simulation results obtained from PSE for basic model is provided in The exhaust gas from CHP model was passed through basic model to analyze the flue gas condensation and heat transfer for district heat network. The pressure loss of flue gas was estimated 0.01 bars. The mass flows of flue gas and DH water was kept constant.

Table 12. The exhaust gas from CHP model was passed through basic model to analyze the flue gas condensation and heat transfer for district heat network. The pressure loss of flue gas was estimated 0.01 bars. The mass flows of flue gas and DH water was kept constant.

Table 12. Simulations results from PSE for basic model.

Flue gas in			Flue gas out			Cold water in			Cold water out			Cond water temp (°C)	Q_trans (kW)
T (°C)	P (bars)	mass flow (kg/s)	T (°C)	P (bars)	mass flow (kg/s)	T (°C)	P (bars)	mass flow (kg/s)	T (°C)	P (bars)	mass flow (kg/s)		
153,75	0,9603	18,64	**55**	0,9503	16,87	50	10	119,4	63,57	9,99	119,4	67,05	6722,59
153,75	0,9603	18,64	**60**	0,9503	17,46	50	10	119,4	60,31	9,99	119,4	67,06	5144,21
153,75	0,9603	18,64	**65**	0,9503	18,27	50	10	119,4	55,86	9,99	119,4	67,06	2920,34

The initial values for exit temperature of flue gas is changed accordingly to perform the simulation of model in IPSEpro PSE. The basic model works according to the principle of counter flow heat exchanger. Therefore, the exit temperature of flue gas could not be lowered than temperature of DH water inlet. The simulation of basic model in IPSEpro indicated that more than 6 MW_{th} of heat energy could be extracted from flue gas due to condensation of water vapor for CHP plant with the fuel input of 55% moisture content.

6.2 Spray tower and Heat pump integration

The schematic of spray tower and heat pump integration in stand-alone CHP plant model is provided in Figure 27. The exhaust gas from CHP plant is directed to spray tower. The district heating water is directed towards two counter-flow heat exchangers. The higher mass flow of DH water is directed towards heat exchanger (htex counter2) and lower mass flow is directed towards another heat exchanger (htex counter3). Heat pump is integrated between lower DH mass flow and htex counter3. The heat pump extracts heat from low temperature DH water. The energy is then transferred to high temperature DH water, which has gained

energy from condensing flue gas in first stage. The main aim is to transfer highest possible energy for district heating water before leaving to district heat condenser (DHC).

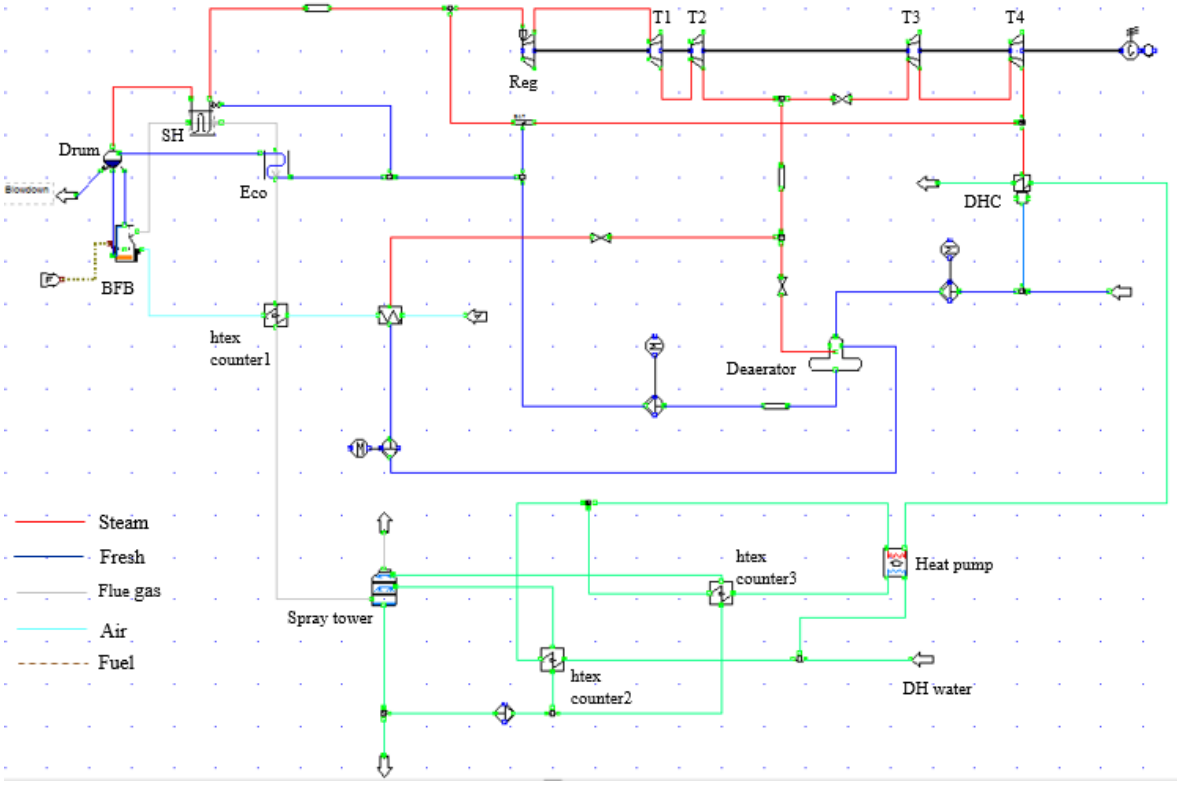

Figure 27. Schematic layout of CHP plant with an integration of spray tower and heat pump in IPSEpro.

The flow of condensate from spray tower is directed towards two heat exchangers. Heat transfer from condensate to higher mass flow DH water is performed in htex counter2 and lower mass flow DH water is carried out in htexcounter3. The approach of temperature difference of 2°C between flue gas exhaust and cooling water has been taken into account in several power plants (Uotila, 2015). In spray tower model, temperature difference of 2°C was approached. To achieve lower temperature of exhaust flue gas and maintain 2°C difference, the temperature of upper scrubber has to be lowered.

Therefore, with the integration of heat pump, the temperature of low DH mass flow was reduced to approximately 34°C. Then the addition of heat exchanger (htex counter3), temperature of upper scrubber was lowered to approximately 43°C. Consequently, temperature of exhaust flue gas was lowered to approximately 45°C. Hence, with the utilization of heat pump, two vital benefits were observed: the temperature of DH water was

raised to approximately 60^{o}C before supplying to DH condenser and temperature of flue gas was lowered significantly by lowering the scrubbing water temperature.

The performance of CHP model with respect to electricity and DH production due to the integration of spray tower and heat pump at constant fuel input is provided in Table 13.

Table 13. Performance of CHP model with the integration of spray tower and heat pump at constant fuel input.

Design Parameters	Stand alone	COP_2	COP_3	COP_4	COP_5	COP_6	COP_7
Fuel (LHV) (MW)	33.362	33.362	33.362	33.362	33.362	33.362	33.362
Net el. (MW)	8.105	8.060	8.066	8.067	8.068	8.069	8.069
DH flow (kg/s)	119.4	183.7	175.3	172.5	171.1	170.3	169.7
DH (MW)	20.000	25.628	24.227	23.760	23.527	23.387	23.293

During simulation of CHP model with the integration of spray tower and heat pump, fuel power and exit temperature of district heating water at DH condenser was kept constant at 90^{o}C. With lower COP, the DH production was higher with compared to higher COP values. The higher heat transfer in heat pump due to low COP raised the raised the supply temperature to DH condenser. In addition, the temperature of DH water exiting the condenser was kept constant i.e. 90^{o}C. Due to these assumptions, the mass flows of DH water were increased in lower COP values.

Next, fuel input was calculated and heating load in DH condenser was kept constant as 20 MW based on the stand-alone CHP model by Saari, J. et al. The initial parameters in design model were kept constant and fuel saving was estimated with FGC and heat pump. Figure 28 provides net production of electricity, DH production with various fuel power and different COP of heat pump. Since DH production in DHC was kept constant, the net DH production increased due to the addition heat transfer in heat pump. Whereas, the electricity production decreased due the consumption of power by the heat pump.

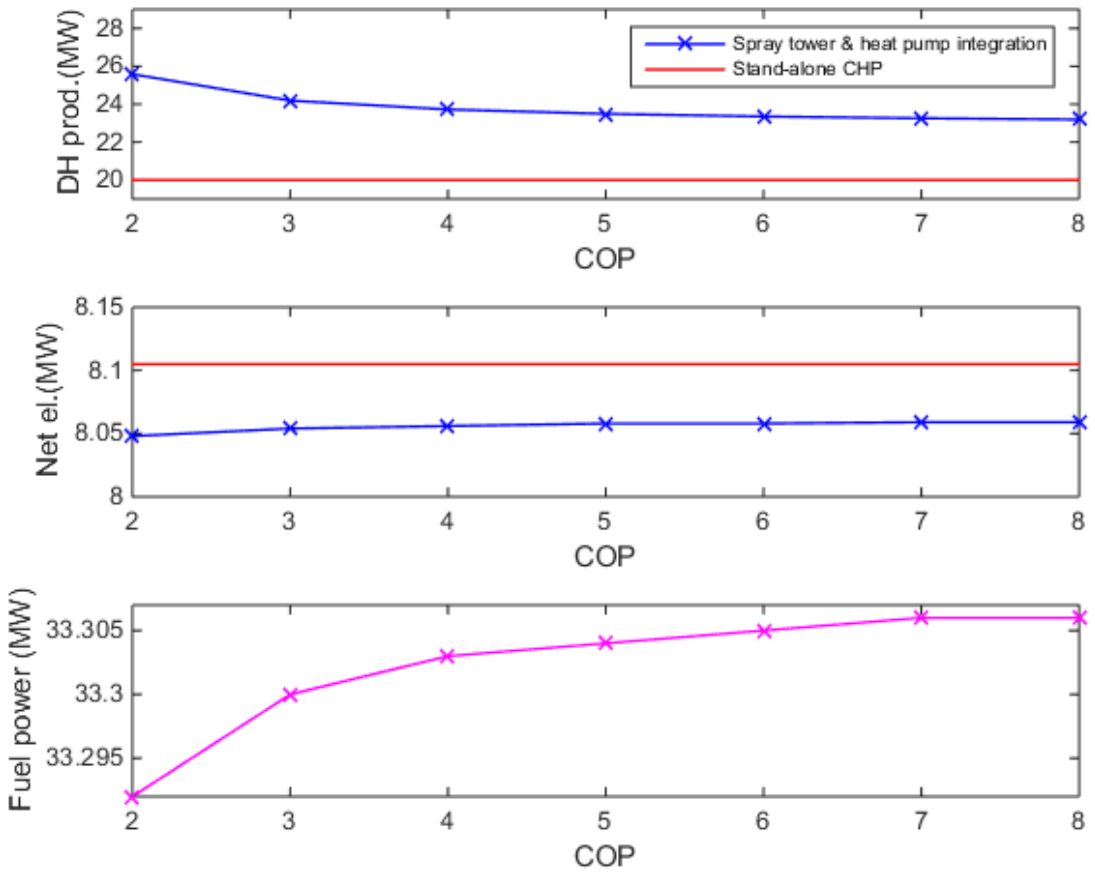

Figure 28. Net electricity, DH production and fuel power with respect do different COP of heat pump.

The DH production was increased significantly whereas, the electricity production decreased. The efficiency diagram of stand-alone CHP and integrated CHP as a function of COP of heat pump is provided in Figure 29. One of the explanation for decline in electricity production is due to the power used by heat pump to operate. Another explanation is due to the higher supply temperature to the DH condenser, which resulted in expansion of steam to higher pressure from the turbine resulting in lower electricity production.

The return temperature of DH water was assumed 50ºC. The supply temperature for both lower and upper scrubber in spray tower were kept low as approximately 52ºC and 43ºC for higher condensation and low-temperature flue gas exit. This was partly carried out by assigning constant value of heat transfer for heat exchangers (htex counter2 and htex counter3).

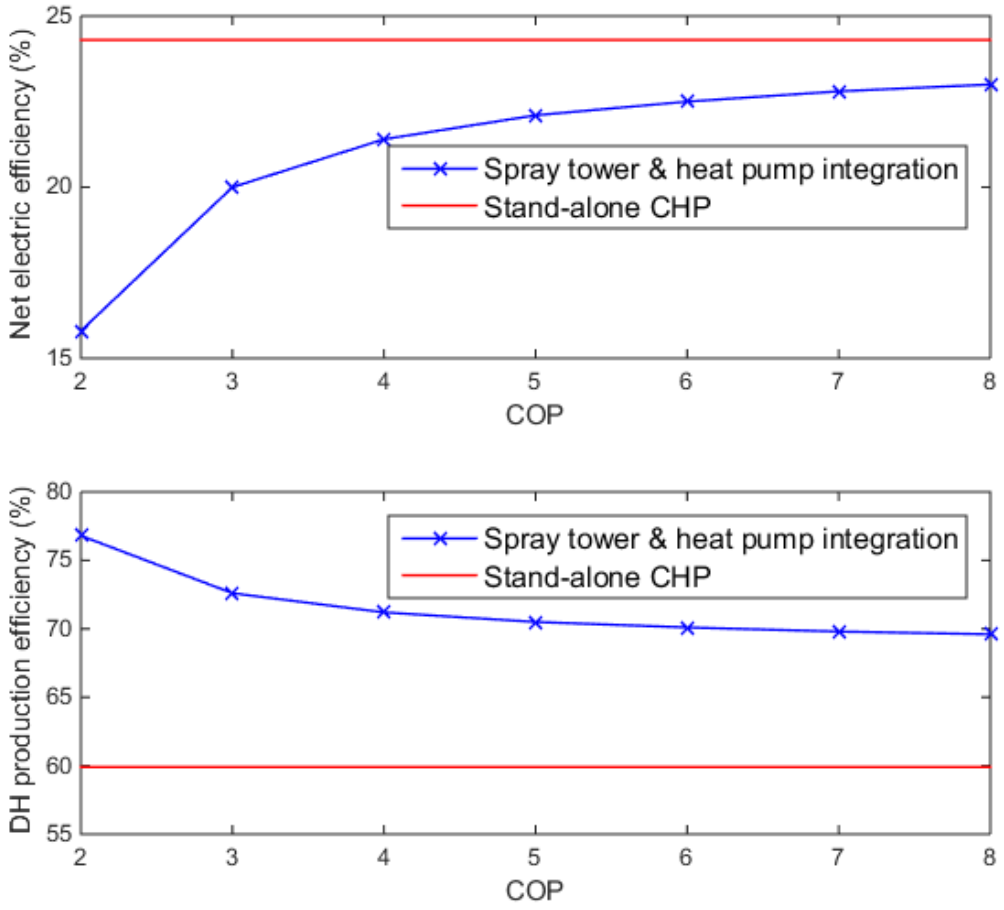

Figure 29. Efficiency of CHP design model and spray tower and heat pump integrated model.

The efficiencies of stand-alone CHP for net electricity production and DH production were 24.3% and 59.9%. The total efficiency of plant was 84.2%. Whereas, with the integration of spray tower and heat pump, the total efficiency was increased to 92.6% accounting the heat production and electricity consumed by the heat pump.

In stand-alone model, the exhaust gas had moisture content of approximately 18.9%. With the integration of spray tower and heat pump at same fuel input, the moisture content was reduced to 7.7%. The total condensation of moisture could not be achieved because condensation of water vapor is restricted by the ability to cool down the flue gas to lower temperature. In addition, when the volumetric water vapor decreases in flue gas, its dew point also decreases significantly (Samuelson, 2008). Therefore, addition of another scrubber could be required for higher amount of condensation.

7 CONCLUSION

This thesis investigated the integration of flue gas condensing unit and heat pump to recover the heat from flue gas. IPSEpro MDK was used to model the FGC and heat pump and, PSE to run the simulation of CHP model. The reference model used for the simulation is based on the stand-alone model developed by Saari, J. et al.

Flue gas condensing is established method adopted by power plant industries for obtaining higher thermal efficiency. FGC is promising technology in CHP plants and research indicates that it has capacity of lowering flue gas emissions below BAT-AELs. It provides vital support to tackle climate change by increasing efficiency of energy plants, saving fuel and reducing the air pollution to the environment. Flue gas condensing is achieved by either using condensing scrubber or tube condenser. Condensing scrubber has higher condensation and emission control properties and condensing in spray tower is core research of this thesis paper. Researches indicate that, spray tower has higher removal efficiencies for gas removal but it is not efficient in removing smaller particles.

The two stage scrubbing is defined in the spray tower model. The primary purpose of lower scrubbing is for the gas removal and upper scrubbing for condensation of water vapor and achieving lower flue gas temperature. However, this thesis paper is entirely based on condensation of water vapor. The estimation of removal of acidic gases and particles are not included. The study on spray tower indicates minimum pressure loss of water. The pressure loss in spray tower in the simulation is estimated 0.2 bars.

Heat pump is prominent technology used in DH networks and provides essential alternative to reduce environmental impacts from CHP plants. The heat pump used in thesis paper is mechanical driven heat pump, which utilizes electricity to operate. In this thesis paper, heat pump is simulated with various values of coefficient of performance and are within the limits of existing values provided in literature review. The modeling of FGC in IPSEpro software is completely based on heat and mass transfer of fluids (water and flue gas). It does not include the pretreatment of flue gases and treatment of wastewater from condensation. The design of heat pump is also based on heat and mass transfer of hot water and specific value for COP is not suggested.

With FGC and heat pump, the return temperature of DH water was raised to approximately 60^{o}C, which resulted in higher temperature and mass flow of water to DH condenser. The

cogeneration efficiency for stand-alone CHP was 84.2% on the LHV basis including DH efficiency (59.9%) and net electricity production efficiency (24.3%). With the integration of spray tower and heat pump, the total efficiency was increased to 92.6%. The DH production efficiency was raised to approximately 70% considering the existing range of COP of heat pump. In both cases, return temperature of DH water was assumed 50^{o}C. However, the net electricity production was lowered to approximately 22%. This was due to the power consumed by heat pump and, expansion of steam to higher pressure from turbine to DH condenser. The simulation on various fuel power flow also indicated that, higher DH production could be obtained with less fuel power than that used in stand-alone CHP model.

The results from simulations estimated the reduction of exhaust gas to the environment and moderate condensation of water vapor in flue gas. In stand-alone CHP model, the exhaust gas temperature was 158^{o}C with moisture content of approximately 18.9%. With FGC, the exhaust gas temperature and moisture content in flue gas were reduced to 45^{o}C and 7.7% respectively.

In conclusion, simulation of FGC model in IPSEpro estimated the increase in thermal and DH production efficiency by the condensation of flue gas and lowered the temperature of exhaust gas from CHP plant. The simulation of integrated spray tower and heat pump CHP model were entirely based on theoretical assumptions of mass and heat transfer. Mechanical losses and energy losses from spray tower and heat pump were not included in the model simulation. Future work on FGC could include all losses and utilization of real-time data from power plants. Further studies on this topic should also include the estimation of removal of particles and acidic gases. The estimation of energy used for treatment of these condensate and effect on overall CHP efficiency should also be included.

8 REFERENCES

Alakangas, E., Koponen, K., Sokka, L. & Keränen, L., 2016. Cascading use and classification of used wood for energy in Finland. *24th European Biomass Conference & Exhibition*, 6-9 June, pp. 118-125.

Axby, F. & Pettersson, C., 2004. *Flue gas condensing with heat pump,* Stockholm: Värmeforsk.

Basu, P., 2015. *Circulating Fluidized Bed Boilers - Design, Operation and maintenance.* Halifax: Springer.

Bisson, T. M. et al., 2013. Chemical-mechanical bromination of biomass ash for mercury removal from flue gases. *Fuel,* Volume 108, pp. 54-59.

Blumberga, D., Vigants, E. & Veidenbergs, I., 2011. Analysis of flue gas condenser operation. *Latvian Journal of Physics and Technical Sciences,* 48(4), pp. 58-65.

Borgnakke, C. & Sonntag, R. E., 2012. *Fundamental of Thermodynamics.* 8th ed. Hoboken: John Wiley & Sons.

Brady, J. & Legatski, L., 1977. Venturi Scrubbers. In: P. N. Cheremisinoff & R. A. Young, eds. *Air Pollution Control and Design Handbook, Part 2.* New York: Marcel Dekker.

Cengel, Y. A. & Boles, M. A., 2015. *THERMODYNAMICS An Engineering Approach.* 8th ed. New York: McGraw-Hill Education.

Cherubini, F. et al., 2011. CO2 emissions from biomass combustion for bioenergy: Atmospheric decay and contribution to global warming. *GCB Bioenergy,* 3(5), pp. 413-426.

Cooper, C. & Alley, F., 1994. *Air Pollution Control: A Design Approach.* 2nd ed. Illinois: Waveland Press Inc..

Cuadrado, R. S., 2009. *Return Temperature Influence of a District Heating Network on the CHP Plant Production Costs,* Gävle: University of Gävle.

David, A. et al., 2017. Heat Roadmap Europe: Large-Scale Electric Heat Pumps in District Heating Systems. *Energies,* 10(4).

Defu, C., Yanhua, L. & Chunyang, G., 2004. Evaluation of retrofitting a conventional natural gas fired boiler into a condensing boiler. *Energy Conversion and Management,* 45(20), pp. 3251-3266.

EC, 2016. *An EU Stratedy on Heating and Cooling,* Brussels: European Commission.

Energiateollisuus, 2018. *District heating in Finland 2017,* Helsinki: Energiateollisuus Ry.

Engineering ToolBox, 2010. *Flue Gas Dew Point Temperatures.* [Online] Available at: https://www.engineeringtoolbox.com/dew-point-flue-gases-d_1583.html [Accessed 04 12 2018].

European Commission, 2017. *Best Available Techniques (BAT) Reference Document for Large Combustion Plants,* Luxembourg: European Union.

FAO, 2004. *Unified Bioenergy Terminology UBET.* Rome: Food and Agriculture Organization of the United Nations.

Garcia, N. P. et al., 2012. *Best availabe technologies for the heat and cooling market in the European Union,* Petten: EU.

GÖTAVERKEN MILJÖ, 2014. *Multifunctional ADIOX® scrubber with condensation/heat pump after semi-dry system.,* Göteborg: GÖTAVERKEN MILJÖ.

Hanna, S. R., 1976. Predicted and observed cooling tower plume rise and visible plume length at the John E. Amos power plant. *Atmospheric Environment,* 10(12), pp. 1043-1052.

Han, X. et al., 2017. Water extraction from high moisture lignite by means of efficient integration of waste heat and water recovery technologies with flue gas pre-drying system. *Applied Thermal Engineering,* Volume 110, pp. 442-456.

Hiltunen, M. & Tang, J., 1988. NOx abatement in Ahlstrom pyropower circulating fluidized bed boilers. In: P. Basu & J. Large, eds. *Circulating fluidized bed technology II.* Oxford: Pergamon Press, pp. 429-436.

Huhtinen, M., Kettunen, A., Nurminen, P. & Pakkanen, H., 1994. *Höyrykattilatekniikka.* 1st ed. Helsinki: Painatuskeskus.

Hutson, N., Krzyzynska, R. & Srivastava, R., 2008. Simultaneous removal of SO2, NOx and Hg from coal flue gas using a NaClO2 - enhanced wet scrubber. *Industrial and Engineering Chemistry Research,* 47(16), pp. 5825-5831.

IEA/FAO, 2017. *How2Guide for Bioenergy,* s.l.: OECD/IEA, FAO.

IEA, 2011. *Techonology Roadmap - Energy-efficient Buildings: Heating and Cooling Equipment*, Paris: IEA.

IEA, 2012. *Technology Roadmap - Bioenergy for Heat and Power,* Paris: International Energy Agency.

IEA, 2016. *World energy balances until 2014,* Paris: International Energy Agency.

IEA, 2018. *IEA - Report.* [Online] Available at: http://www.iea.org/statistics/statisticssearch/report/?country=WORLD&product=renewablesandwaste&year=2015
[Accessed 14 May 2018].

Incropera, F. P., Dewitt, D. P., Bergman, T. L. & Lavine, A. S., 2007. *Fundamentals of Heat and Mass Transfer.* 6th ed. Hoboken: John Wiley $ Sons, Inc..

IPCC, 2011. *IPCC Special Report on Renewable Energy Sources and Climate Change Mitigation,* New York: Cambridge University Press.

IPCC, 2018. *Global Warming of 1.5oC - Summary for Policymakers,* Geneva: World Meteorological Organization.

Jeong, K., Kessen, M. J., Bilirgen, H. & Levy, E. K., 2010. Analytical modeling of water condensation in condensing heat exchanger. *International Journal of Heat and Mass Transfer,* 53(11-12), pp. 2361-2368.

Jones, J. M. et al., 2014. *Pollutants Generated by the Combustion of Solid biomass Fuels*. London: Springer.

Kaltschmitt, M. & Hartmann, H., 2001. *Energie aus Biomasse:*. Berlin: Springer-Verlag Berlin heidelberg.

Kohl, A. & Nielsen, R., 1997. *Gas Purification.* 5th ed. Houston: Gulf Publishing Company.

Lee, B.-K., Jung, K.-R. & Park, S.-H., 2008. Development and application of a novel swirl cyclone scrubber-(1) Experimental. *Journal of Aerosol Science,* 39(12), pp. 1079-1088.

Mussatti, D. & Hemmer, P., 2002. *EPA AIR POLLUTION CONTROL COST MANUAL*. 6th ed. North Carolina: United States Environmental Protection Agency.

Obernberger, I., Brunner, T. & Bärnthaler, G., 2006. Chemical properties of solid biofuels - significance and impact. *Biomass and Bioenergy,* 30(11), pp. 973-982.

OECD/IEA, 2017. *Technology Roadmap: Delivering Sustainable Bioenergy,* s.l.: International Energy Agency.

OECD/IEA, 2018. *Renewables Information*, Paris: International Energy Agency.

Pak, S. & Chang, K., 2006. Performance estimation of a Venturi scrubber using a computational model for capturing dust particles with liquid spray. *Journal of Hazardous Materials,* 138(3), pp. 560-573.

Park, S. et al., 2005. Wet scrubbing of poly disperse aerosols by freely falling droplets. *Journal of Aerosol Science,* Volume 36, pp. 1444-1458.

Passi, P., Kontu, K., Rinne, S. & Ruohonen, S., 2016. *Large heat pumps in district heating systems,* Helsinki: VALOR.

Pence, M., 2012. *Handbook of Air Pollution Control Systems and Devices.* 1st ed. Delhi: University Publications.

Qin, K. & Thunman, H., 2015. Diversity of chemical composition and combustion reactivity of various biomass fuels. *Fuel,* Volume 147, pp. 161-169.

Saari, J. et al., 2016. Integration of hydrothermal carbonization and a CHP plant: Part 2 - operational and economic analysis. *Energy,* Volume 113, pp. 574-585.

Samuelson, C., 2008. *Recovery of water from boiler flue gas,* Bethlehem: Lehigh university.

Sayegh, M. A. et al., 2018. Heat pump placement, connection and operational modes in European district heating. *Energy and Buildings,* Volume 166, pp. 122-144.

Selivanovs, J. et al., 2017. Flue gas treatment multi-criteria analysis. *Energy Procedia,* Volume 128, pp. 379-385.

Shuangchen, M. et al., 2017. Environmental influence and countermeasures for high humidity flue gas discharging from power plants. *Renewable and Sustainable Energy Reviews,* Volume 73, pp. 225-235.

Singh, R. & Shukla, A., 2014. A review on methods of flue gas cleaning from combustion of biomass. *Renewable and Sustainable Energy Reviews,* Volume 29, pp. 854-864.

Sullivan, A. & Ball, R., 2012. Thermal decomposition and combustion chemistry of cellulosic biomass. *Atmospheric Environment,* Volume 47, pp. 133-141.

Szulc, P. & Tietze, T., 2017. Recovery and energy use of flue gas from coal power plant. *Journal of Power Technologies,* 97(2), pp. 135-141.

Tassou, S. A., 1988. Heat recovery from sewage effluent using heat pumps. *Heat Recovery Systems and CHP,* 8(2), pp. 141-148.

Teppler, M., Wood, J. & Buzzell, P., 2017. *Flue gas condensate and energy recovery,* Västerås, Sweden: Radscan Intervex AB.

Terhan, M. & Comakli, K., 2016. Design and economic analysis of a flue gas condenser to recover latent heat from exhaust flue gas. *Applied Thermal Engineering,* Volume 100, pp. 1007-1015.

Uotila, J., 2015. *Heat recovery and environmental impacts of flue gas condensing,* Espoo: Aalto University.

Vakkilainen, E. K., 2017. *Steam Generation from Biomass - Construction and Design of Large Boilers.* Amsterdam: Butterworth-Heinemann.

Wark, K., Warner, C. & Davis, W., 1998. *Air Pollution: Its Origin and Control.* 3rd ed. Reading, MA: Addison-Wesley.

Vehlow, J. & Dalager, S., 2010. Incineration: Flue gas cleaning and emissions. In: T. H. Christensen, ed. *Solid Waste Technology & Management, 1 & 2.* Chichester: John Wiley & Sons Ltd, pp. 393-420.

Veidenbergs, I., Blumberga, D., Vigants, E. & Kozuhars, G., 2010. Heat and Mass Transfer Process in Scrubber of Flue Gas Heat Recovery Device. *Environmental and Climate Technologies,* 4(1), pp. 109-115.

Wendt, J. O., Linak, W. P., Groff, P. W. & Srivastava, R. K., 2001. Hybrid SNCR-SCR technologies for NOx control: Modeling and Experiment. *AlChE Jounal,* 47(11), pp. 2603-2617.

Werner, S., 2017. International review of district heating and cooling. *Energy,* Volume 137, pp. 617-631.

Yin, C., Rosendahl, L. A. & Kær, S. K., 2008. Grate-firing of biomass for heat and power production. *Progress in Energy and Combustion Science*, 34(6), pp. 725-754.

Zhelev, T. & Semkov, K., 2004. Cleaner flue gas and energy recovery through pinch analysis. *Journal of Cleaner Production,* 12(2), pp. 165-170.

Zhuang, Y. et al., 2015. Experimental study of formation mechanism of stack rainout from coal-fired power plant. *China Environmental Science,* 35(3), pp. 714-722.

Appendix 1 Stand-alone CHP parameters in IPSEpro model

Φ_{fuel}	*MW*	*33.36*
$\Phi_{boiler,th}$	*MW*	*28.92*
$q_{m,fuel}$	*kg/s*	*4.49*
$q_{m,air}$	*kg/s*	*14.31*
q_{DH}	*kg/s*	*119.4*
$q_{m,FG}$	*kg/s*	*18.77*
$q_{m,turbine}$	*kg/s*	*10.89*
P_{gen}	*MW*	*8.79*
$P_{el,net}$	*MW*	*8.11*
P_{DH}	*MW*	*20.0*
$P_{el,\ pumps}$	*MW*	*0.17*
$P_{el,\ aux}$	*MW*	*0.51*
p_{FW}	*bar*	*102.4*
p_{drum}	*bar*	*100.3*
$p_{T1,\ in}$	*bar*	*60.8*
$p_{T4,\ out}$	*bar*	*0.8*
p_{DHC}	*bar*	*10*
$HHV_{woodchips}$	*MJ/kg*	*20.91*
$LHV_{woodchips}$	*MJ/kg*	*7.43*
T_{stack}	^oC	*158.15*
T_{furn}	^oC	*892.31*
η_{boiler}	*%*	*86.50*
η_{el}	*%*	*24.3*
η_{DH}	*%*	*59.9*
η_{total}	*%*	*84.2*

Appendix 2 Integrated CHP parameters in IPSEpro model

Φ_{fuel}	*MW*	*33.31*
$\Phi_{boiler,th}$	*MW*	*28.87*
$q_{m,fuel}$	*kg/s*	*4.48*
$q_{m,air}$	*kg/s*	*14.29*
q_{DH}	*kg/s*	*170.1*
$q_{m,FG}$	*kg/s*	*16.48*
$q_{m,turbine}$	*kg/s*	*10.87*
P_{gen}	*MW*	*8.74*
$P_{el,net}$	*MW*	*8.06*
P_{DH}	*MW*	*23.35*
$P_{el,pumps}$	*MW*	*0.17*
$P_{el,aux}$	*MW*	*0.51*
p_{FW}	*bar*	*102.4*
p_{drum}	*bar*	*100.3*
$p_{T1,in}$	*bar*	*60.7*
$p_{T4,out}$	*bar*	*0.83*
p_{DHC}	*bar*	*9*
$HHV_{woodchips}$	*MJ/kg*	*20.91*
$LHV_{woodchips}$	*MJ/kg*	*7.43*
T_{stack}	*^oC*	*45*
T_{furn}	*^oC*	*891.93*
η_{boiler}	*%*	*86.50*
η_{el}	*%*	*22.5*
η_{DH}	*%*	*70.1*
η_{total}	*%*	*92.6*
Heat pump		
COP_{HP}	-	*6*
W_{HP}	*kW*	*558.22*
$Q_{trans,HP}$	*MW*	*3.35*
Spray tower		
dp	*bar*	*0.2*
T_{sw1}	*^oC*	*52*
T_{sw2}	*^oC*	*43*
T_{cond}	*^oC*	*64.65*
q_{sw1}	*kg/s*	*71.11*
q_{sw2}	*kg/s*	*45.02*
q_{cond}	*kg/s*	*118.4*